



# Self-powered wearable sensing devices for digital health

Cite this: DOI: 10.1039/d5mh00443h

Yumeng Zhang,<sup>†ab</sup> Engui Wang,<sup>†ab</sup> Han Ouyang<sup>\*ab</sup> and Zhou Li <sup>\*ab</sup>Received 12th March 2025,  
Accepted 20th May 2025

DOI: 10.1039/d5mh00443h

rsc.li/materials-horizons

Self-powered wearable sensing devices are portable devices that convert environmental stimuli like light, heat, mechanical motion, and more into electrical signals to achieve health monitoring and data collection functions. Due to the flexibility, portability, and ability to combine with smart AI, self-powered wearable sensors are extensively utilized in digital health. This review focuses on self-powered wearable sensing devices that utilize human energy, introducing their power supply mechanism and efficiency improvement methods. It also provides an overview of the common structural and morphological features of self-powered wearable sensors currently used in healthcare. Besides, the specific applications of self-powered wearable sensors in digital healthcare are summarized. Finally, the technical bottlenecks, application prospects, and possible improvement strategies are discussed.

## Wider impact

Self-powered wearable sensors effectively address the bulkiness of digital health devices caused by external power sources, thanks to their portability and sustainability. However, their development faces significant challenges due to power efficiency issues in self-powered mechanisms and the varying impacts of different device forms on energy harvesting efficiency. Continuous optimization of power supply mechanisms and the integration of various power supply methods can enhance power supply efficiency. Additionally, thoughtful design that aligns with human anatomy and meets patient needs can significantly improve energy harvesting. A thorough understanding of power supply mechanisms and the application scenarios for different device forms is essential for advancing self-powered wearable sensors. This article provides a detailed overview of the various power supply mechanisms for these sensors and methods to enhance their energy output performance. It also explores the application and development prospects of devices with diverse structural forms, highlighting their role in digital health. The insights presented aim to equip researchers with a comprehensive understanding of the latest advancements in self-powered wearable sensors and inform future developments in this field.

## 1. Introduction

With the increasing prevalence of global health and medical challenges, the quest for effective healthcare solutions to create robust and reliable disease defense mechanisms has gained global attention.<sup>1,2</sup> Digital medical devices are essential in this field, as they can integrate multiple functions and offer real-time visual feedback which enables users to understand their health status better. Digital medical devices can effectively monitor various health indicators such as heart rate, pulse, and sleep quality, providing users with comprehensive health data analysis. The fundamental digital healthcare device is the

multifunctional watch that monitors heartbeats and pulse rate.<sup>3</sup> This trend not only enhances individuals' ability to manage their health but also provides richer data support for medical professionals to make more accurate diagnoses and treatments. With recent advancements in artificial intelligence (AI), the potential for these digital health devices to become smarter, more multifunctional, and seamlessly integrated into daily life is promising.<sup>4,5</sup> The application of AI enables these devices to analyze records in real-time, deliver personalized medical recommendations, and even predict potential health problems in certain situations. In addition, the portability of devices has become particularly important to ensure that users can easily use these tools in their daily lives, thereby continuously monitoring and managing their health. These properties are expected to drive the progression of personalized health. In particular, wearable sensors that fulfill these criteria are setting the standard and paving the way for innovative digital healthcare applications, ultimately transforming health monitoring and management.<sup>6,7</sup>

<sup>a</sup> Beijing Institute of Nanoenergy and Nanosystems, Chinese Academy of Sciences, Beijing 101400, China. E-mail: zli@binn.cas.cn

<sup>b</sup> School of Nanoscience and Engineering, School of Chemical Sciences, University of Chinese Academy of Sciences, Beijing 100049, China.

E-mail: ouyanghan@ucas.ac.cn

<sup>†</sup> These authors contributed equally.

Sensors have a long history, dating back to Warren Johnson's 1883 invention, which measured room temperature and later evolved into the thermostat.<sup>8</sup> Today, "smart sensors" encompass advanced devices that not only detect various physical properties but also achieve digital data conversion and upload to cloud systems.<sup>9,10</sup>

In the 1960s, wearable technology—focusing on devices that can be worn directly on the body or integrated into clothing and accessories—was an innovative concept first introduced by the MIT Media Lab. Subsequently, two MIT mathematics professors, Edward Thorp and Claude Shannon, designed and built the world's first wearable computer. Subsequently, wearable sensing devices combining wearable technology and smart sensors can harvest physiological signals to prevent or cure disease.<sup>1,11,12</sup> The concept of personalized medicine is rapidly developing, and more and more people hope to meet their unique health needs through technological means. Wearable sensors, as an essential component of this process, stand out due to their ability to simultaneously meet multiple functional requirements.<sup>13</sup> By connecting with mobile applications, these devices can synchronize data in real-time, providing in-depth health insights and recommendations, thereby enhancing users' health awareness.<sup>14</sup> These sensors not only provide accurate data collection but also assist users in effective health management through intelligent analysis. As sensors evolve, their performance improves and their energy requirements increase, it has become significant to develop sensors that do not require an external energy supply.

In response to this need, scientists have begun experimenting with various power generation techniques to harvest various forms of energy from human movement as well as from the surrounding environment to power sensors. Self-powered wearable sensors have been widely utilized since Wang *et al.* created Triboelectric Nanogenerators (TENGs).<sup>15</sup> Along with the development of new forms of TENGs,<sup>16,17</sup> piezoelectric nanogenerators (PENGs)<sup>18</sup> and pyroelectric nanogenerators (PyNGs)<sup>19,20</sup> come into sight; for example, the device for motor function recovery after nerve injury can be worn daily and no longer needs an additional power supply.<sup>21</sup> Despite these advances, improving energy conversion efficiency remains a significant challenge. Theoretically, TENGs can achieve total efficiencies reaching up to 85%.<sup>22</sup> Similarly, PENGs have demonstrated theoretical efficiencies as high as 66%.<sup>23</sup> However, in practical scenarios, the actual energy conversion efficiency is often much lower, typically below 30%. For example, the multi-layer TENG for energy harvesting developed by Zheng *et al.*<sup>24</sup> achieved a conversion efficiency of 24.89%, while the PENG reported by Rasappan *et al.*<sup>25</sup> demonstrated an efficiency of only 5.4%. Table 1 presents the energy produced by specific physiological activities of humans and the power density of the related energy harvesting technology.

In recent years, self-powered wearable sensing devices have experienced unpredictable growth (Fig. 1). The applications in digital healthcare include physical signal monitoring, illness cures, and so on. With the continuous advancement of AI and deep learning, we have reason to believe that future digital

**Table 1** Various biological energies of the human body and their energy harvesting technologies

Energy source	Energy supply (W)	Energy harvesting technology	Power density (mW cm <sup>-2</sup> )
Body heat <sup>26</sup>	60–180	TEG <sup>27</sup>	$6.8 \times 10^{-3}$
		TEG <sup>28</sup>	3.32
Arm motion <sup>29</sup>	60	TENG <sup>30</sup>	$6 \times 10^{-4}$
		TENG <sup>31</sup>	$3.062 \times 10^{-2}$
		TENG <sup>32</sup>	$8.5 \times 10^{-3}$
		TENG <sup>33</sup>	30.96
		TENG <sup>34</sup>	$2.75 \times 10^{-7}$
Footfall <sup>29</sup>	67	PENG <sup>35</sup>	$5.625 \times 10^{-2}$
Exhalation <sup>29</sup>	1	TENG <sup>36</sup>	$0.12 \times 10^{-3}$
Heart beat <sup>29</sup>	1.4	EHU <sup>37</sup>	$9.24 \times 10^{-3}$



**Fig. 1** Self-powered wearable sensing devices of different power supply methods. TENG. Reproduced with permission from ref. 41–43. Copyright 2022 The Authors. Advanced Science published by Wiley-VCH GmbH. Copyright 2024 Elsevier Ltd. All rights are reserved, including those for text and data mining, AI training, and similar technologies. Copyright 2024 The Authors. Advanced Science published by Wiley-VCH GmbH. PENG. Reproduced with permission from ref. 44–46. Copyright 2022 The Authors. Publishing Services by Elsevier B.V. on behalf of KeAi Communications Co. Ltd. Copyright 2022, American Chemical Society. Copyright 2022 Wiley-VCH GmbH. TED. Reproduced with permission from ref. 47–49. Copyright 2022, The American Association for the Advancement of Science. Copyright 2024, The Author(s). Copyright 2024 Wiley-VCH GmbH. BFC. Reproduced with permission from ref. 50–52. Copyright 2024, American Chemical Society. Copyright 2024, The Author(s), under exclusive licence to Springer Nature Limited. Copyright 2024 Wiley-VCH GmbH.

medical devices will become more intelligent, providing people with more comprehensive health protection and support.<sup>38</sup> However, with this improvement comes a critical challenge: the need for more power. Enhanced functionalities demand greater energy output, making it essential to develop self-powered wearable sensors that can sustain prolonged use without frequent recharging.<sup>39</sup> Self-powered wearable sensing devices can simultaneously utilize energy from the external environment and the human body. The energy expenditure of typical physiological activities includes approximately 1 W for one breath,<sup>29</sup> 1.4 W for one heartbeat,<sup>29</sup> and around 100 W for

Table 2 Comparisons of various self-powered flexible wearable sensing devices

Energy source	Capacity (kPa)	Sensitivity	Power density (mW cm <sup>-2</sup> )
Triboelectric <sup>53</sup>	55.6	—	1.4784 × 10 <sup>-3</sup>
Triboelectric <sup>54</sup>	301358.5	—	3 × 10 <sup>-4</sup>
Triboelectric <sup>55</sup>	60	7.989 V kPa <sup>-1</sup>	—
Triboelectric <sup>56</sup>	900	2.54 V kPa <sup>-1</sup>	—
Piezoelectric <sup>57</sup>	75	—	3.15 × 10 <sup>-3</sup>
Piezoelectric <sup>58</sup>	—	—	13
Piezoelectric <sup>59</sup>	600	0.0598 V N <sup>-1</sup>	—
Piezoelectric <sup>60</sup>	10	18.376 kPa <sup>-1</sup>	—
Thermoelectric <sup>61</sup>	—	—	11.14
Fuel cell <sup>62</sup>	—	—	2.26 × 10 <sup>-3</sup>
Fuel cell <sup>63</sup>	—	—	13 × 10 <sup>-3</sup>
Electromagnetism <sup>64</sup>	226.4	139.4 μA	—
Electrochemistry <sup>65</sup>	—	—	82.5
Electrochemistry <sup>66</sup>	—	96.6 μA mM <sup>-1</sup> cm <sup>-2</sup>	—
Electrochemistry <sup>67</sup>	—	592 μA mM <sup>-1</sup>	—
Piezoelectric + photoelectricity <sup>68</sup>	150	0.101 kPa <sup>-1</sup>	—

the total sensible heat released into the atmosphere while walking at a natural speed.<sup>26</sup> Despite decades of exploration, the conversion efficiency of existing human energy harvesting technologies remains relatively low, typically achieving power levels ranging from microwatts to milliwatts.<sup>29</sup> From Table 1, we see human energy conversion in specific usage scenarios. In addition, the energy consumption of some common electronic devices, such as biosensors used for continuous monitoring, typically has a power of 0.5–5 mW, while the maximum power of low-power Bluetooth is 5–15 mW. There are many reasons for this situation. To solve this dilemma, innovation in energy capture technologies such as solar energy, thermal energy, and kinetic energy capture is crucial. In addition, the development of self-powered equipment materials<sup>10</sup> and manufacturing processes<sup>40</sup> is also necessary to ensure power output. As we look to the future, the synergy between advanced technology and energy efficiency will be vital in shaping the landscape of digital healthcare.

In this review, we examine the application and development of various power supply methods for self-powered wearable sensing devices in digital health. Additionally, we identify areas for future improvement, including enhanced energy output and better integration with user needs, providing insights for further advancements in this field (Table 2).

## 2. Principle of power supply for self-powered wearable sensing devices

In the short term, self-powered sensing devices and systems that utilize displacement current have garnered significant attention for their capacity to transfer biomechanical or heat energy into electrical power for a variety of applications.<sup>69</sup> This self-powered technology enables wearable sensors to facilitate real-time monitoring while ensuring long-term use without the need for frequent battery replacements or re-implantation.<sup>70</sup> Common power supply modes cover triboelectric (Fig. 2(a)),<sup>11,12,71–77</sup> piezoelectric (Fig. 2(b)),<sup>18,21,78–80</sup> thermoelectric (Fig. 2(c)),<sup>81–83</sup> and other modes, like biofuel cells (Fig. 2(d))<sup>84–86</sup> and magnetoelectric,<sup>64</sup> hybrid power supply.<sup>87–90</sup>

Each type of energy-harvesting device based on displacement current offers unique advantages, but they also come with practical limitations that must be considered.<sup>8</sup>

As technology advances and the demand for medical care increases, self-powered wearable sensors have become multifunctional. This means it is necessary to improve the power supply efficiency of the self-powered mechanism. Researchers have been actively investigating various power supply methods to improve the accuracy and sensitivity of these sensors, aiming to enhance their overall performance and usefulness in monitoring health metrics.<sup>91</sup> In this section, the principle of every power supply mode is introduced. Besides, this section also contains strategies for improving power supply efficiency.

### 2.1 Triboelectric effect

According to the quantified triboelectric series diagram, the contact and separation of two materials with differences in sorting will lead to charge transfer and generate triboelectricity. Since Wang<sup>15</sup> first combined the triboelectric effect and electrostatic induction to develop TENGs, it has become a self-powered device with a wide range of applications. A TENG has four working methods: vertical contact-separation mode<sup>11,71,73,76</sup> which is the most common, lateral sliding mode, single-electrode mode,<sup>72</sup> and freestanding triboelectric-layer mode (Fig. 2(a)).<sup>12</sup> Due to its small size, flexibility, and high power efficiency, TENG has become an important power source for wearable sensors.<sup>92,93</sup> TENGs still face challenges with the power supply of wearable sensors. The main issue is the power supply efficiency. When considering portability and a broader range of application scenarios, TENGs can supply adequate energy for self-powered wearable sensing devices while meeting miniaturization requirements. However, TENG's high voltage and low current output characteristics present challenges for these devices in practical applications.<sup>94</sup> Enhancing power supply efficiency involves improving triboelectric material performance<sup>71–73,75</sup> and optimizing TENG's structure (Table 3).<sup>11,74,76</sup>

In different cases, we need TENG's structure to change both inside and outside. TENG's structure includes the friction layer

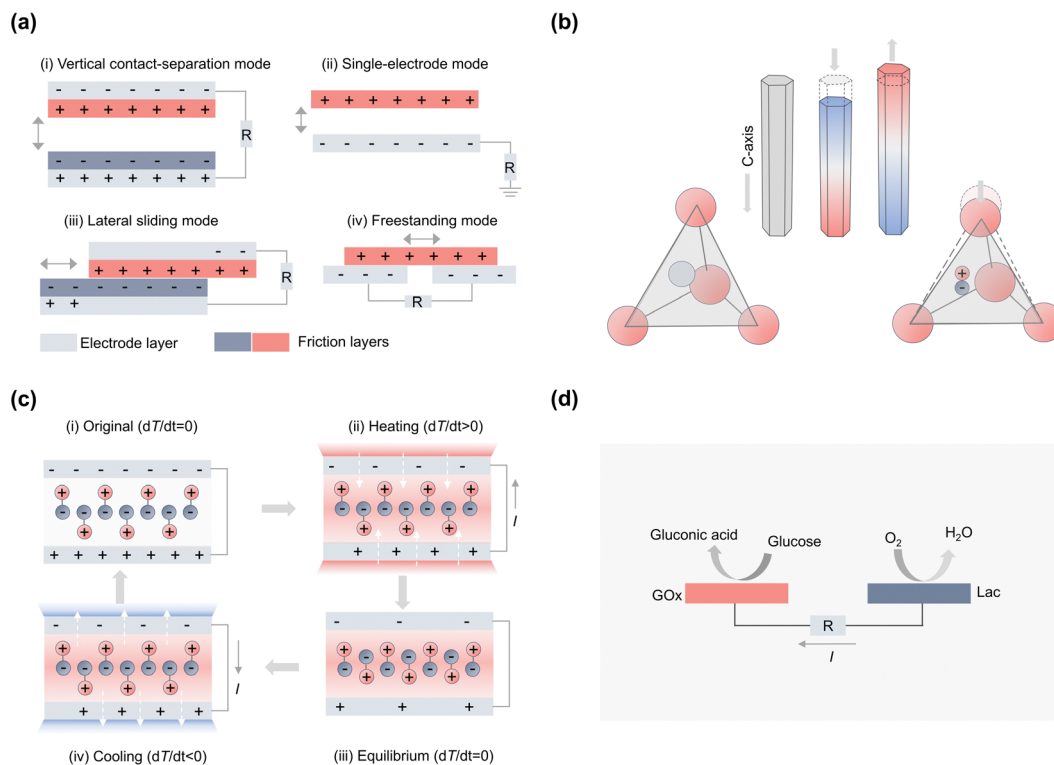


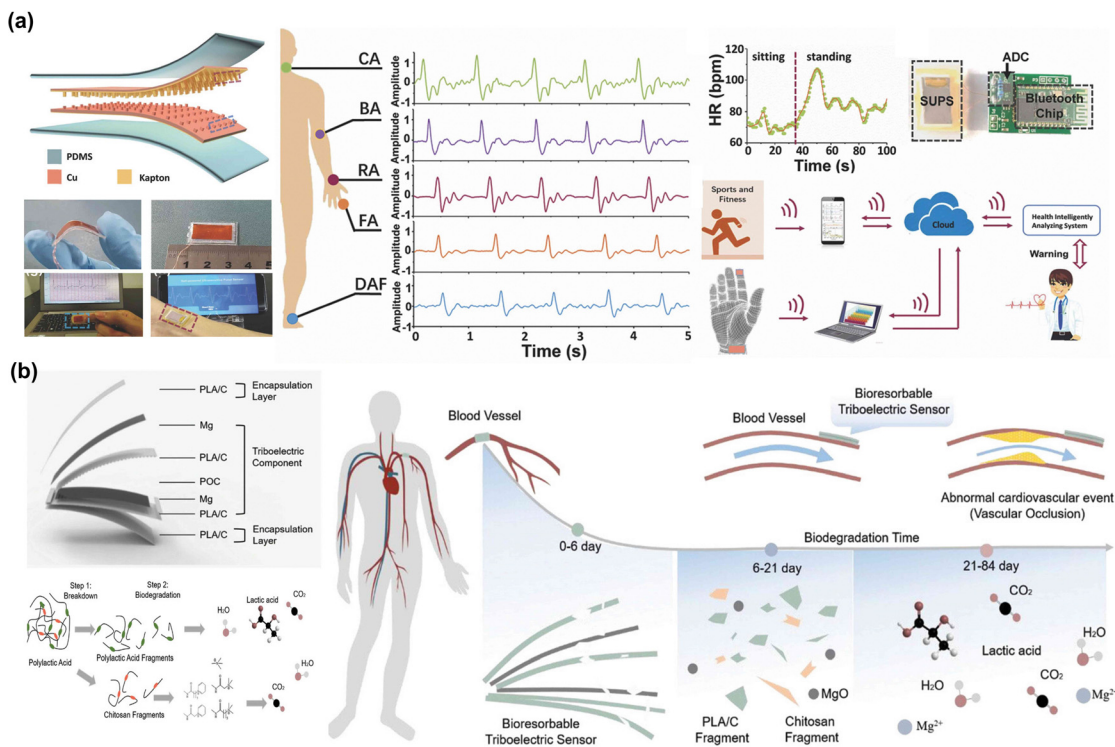
Fig. 2 Schematic diagram of self-powered mechanism. (a) TENG's four modes. (i) Vertical contact-separation mode. (ii) Lateral sliding mode. (iii) Single-electrode mode. (iv) Freestanding triboelectric-layer mode. (b) PENG's principle. (c) Thermoelectric effect. (d) Biofuel cell's principle.

Table 3 Electrical properties of TENGs of different sizes

Material	Dimension	Electrical properties
MXene/polymethyl methacrylate <sup>95</sup>	3 cm <sup>2</sup>	37.8 V, 1.8 μA, 14.1 nC, 7.3 μW
Thermoplastic urethane/AgNWs <sup>30</sup>	4 cm <sup>2</sup>	95 V, 0.3 μA, 6000 μW m <sup>-2</sup>
PTFE/(chitosan/glycerol) <sup>96</sup>	4 cm <sup>2</sup>	25 V, 1 μA
Chitosan/fluorinated ethylene propylene <sup>97</sup>	4 cm <sup>2</sup>	74.1 V, 1.71 μA, 20.5 nC
Polycaprolactone/Ag <sup>98</sup>	5 cm <sup>2</sup>	7.2 V, 0.6 μA, 12 nC
Kapton/polyethylene terephthalate <sup>99</sup>	10 cm <sup>2</sup>	6.0 V, 2.3 nC
Perfluoroalkoxy/Au <sup>100</sup>	16 cm <sup>2</sup>	2.4 V, 156 μA
PDMS/AgNWs <sup>101</sup>	25 cm <sup>2</sup>	43 V, 0.28 μA
PDMS/elastomer <sup>72</sup>	12 cm <sup>2</sup>	145 V, 35 000 μW m <sup>-2</sup>
(Polyethylene oxide/polypropylene glycol)/(polycaprolactone/ethyl cellulose) <sup>75</sup>	0.90625 cm <sup>3</sup>	6.30 V, 0.07205 μA, 2.12 nC, 2.25 μW m <sup>-2</sup>
PTFE/Al <sup>53</sup>	3.78 cm <sup>3</sup>	11.45 V, 4.46 μA, 10.56 μW cm <sup>-3</sup>
PDMS/polyvinyl chloride <sup>102</sup>	42.39 cm <sup>3</sup>	672 V, 15.6 μA, 79.8 nC, 3320 μW

and the mechanical structure.<sup>74</sup> Adding multiple friction layers to increase triboelectric sources can support multifunctional sensors. Besides, by changing the shape of the friction layer, the friction power supply can also be increased to provide output (Fig. 3(a)).<sup>103</sup> A flexible self-powered ultrasensitive pulse sensor was designed to stem from this principle. Adapting to different application scenarios, the mechanical structure of TENGs alters flexibly. To better utilize the water energy, a gas-liquid two-phase flow-based TENG is designed by Dong *et al.*<sup>74</sup> The gas-liquid two-phase flow-based TENG utilizes a capillary tube stretch into a water tank. On top of the tube is a lateral polytetrafluoroethylene (PTFE) tube, and a porous reticulated electrical conductive titanium (Ti) electrode is at the

end of the PTFE tube. When gas flows through the PTFE tube, a negative pressure appears in the cross of two tubes, lifting the water. The sucked water collides with the tube wall and is dispersed and atomized. The PTFE tube, porous mesh conductive Ti electrode, and water construct the closed loop. Similarly, changes in microstructure can also help increase the power of TENGs to some extent.<sup>104</sup> The triboelectric effect relies on the surface interaction between two different electronegative materials. Increasing the roughness of the surface can enhance the friction of the materials.<sup>71</sup> The bioresorbable triboelectric sensor shown in Fig. 3(b) consists of two frictional layers that transform mechanical movement signals into electrical signals.<sup>11</sup> A poly(lactic acid) and 4% chitosan film that features



**Fig. 3** The application of TENG in cardiovascular diseases. (a) The structure and pulse signal output of self-powered ultrasensitive pulse sensors, as well as the wireless health monitoring system images. Reproduced with permission from ref. 103 Copyright 2017 WILEY-VCH Verlag GmbH & Co. KGaA, Weinheim. (b) Biodegradable triboelectric sensor schematic diagram and structure. Illustration of biodegradation for poly(lactic acid)–(chitosan 4%) polymer. Reproduced with permission from ref. 11. Copyright 2021 Wiley-VCH GmbH.

a nanostructured surface acts as the frictional layer. The back-side features a magnesium (Mg) layer as an electrode. Additionally, Mg has been deposited on another poly(lactic acid) and 4% chitosan sheeting to create a nanostructured metal layer that functions as both an electrode and a frictional layer. The entire device is encapsulated in poly(lactic acid) and 4% chitosan, with a flexible poly(1,8-octane diol *co*-citric acid) used as an adhesive. Surface nanostructures can enhance the effective contact part of the friction layer during operation, resulting in stronger electrical signals that improve sensor sensitivity. The open circuit voltage of the TENG reaches up to 65.2 V. Improving triboelectric materials' performance can effectively enhance the power supply efficiency. In addition to changing TENG's structure, an external charge excitation circuit can also increase output.<sup>76</sup> These three methods fit TENGs to different self-powered wearable sensors.

To improve triboelectric materials' performance, the effective methods widely used involve material optimization<sup>73,75</sup> and adjusting the material's surface texture.<sup>71</sup> One common method for material optimization is to enhance their charge storage capacity in an electric field through the doping of conductive materials. This process reduces internal impedance to promote efficient charge transfer, reduces energy loss, and improves current output. In the preparation of biodegradable TENGs, according to triboelectric polarities, polyethylene oxide and polycaprolactone are commonly used tribopositive and tribonegative layer materials, respectively. Their triboelectric

polarities are related to the types of main- or side-chain chemical groups or group densities. Li *et al.*<sup>75</sup> doped small amounts of poly(propylene glycol) and ethyl cellulose to enhance the output performance of biodegradable TENGs. They utilize vertical contact-separation mode and prepare poly(trimethylene carbonate) as the encapsulation layer, Mg as the electrode, doped polyethylene oxide/poly(propylene glycol) as the tribopositive layer, and doped polycaprolactone/ethyl cellulose as the tribonegative layer. This biodegradable TENG can adhere to the abdomen and sensitively recognize breathing patterns. The test open circuit voltage of a biodegradable TENG is 6.30 V, while during breath detection, the maximum open circuit voltage is 2.85 V. The main reason for this difference is that the respiratory intensity of the human body cannot reach the strength of the testing equipment. Besides doping, surface modification<sup>97</sup> and developing new triboelectric materials<sup>72</sup> can also work. Surface modifications, including chemical treatments and plasma treatment, can enhance the stability of the triboelectric effect and lessen the impact of the external environment on TENG performance. Han *et al.*<sup>97</sup> designed a novel TENG based on the chitosan film. In the experiment, chitosan TENGs based on different processing methods (such as smoothing, imitating sandpaper texture, and electrospinning treatment) showed that surface structure changes significantly improved voltage, current, and electricity output, with electrospinning treatment performing the best. Besides, the output performance of the vertical contact-separation TENG is

greatly enhanced due to the significant increase in the effective contact area between the two friction materials, with chitosan and fluorinated ethylene propylene film being used as the positive and negative friction materials, respectively. Improving the performance of triboelectric materials boosts the efficiency and stability of TENGs while promoting green energy technology and expanding applications in smart devices and self-powered systems.

TENG is a common power supply device. Researchers have implemented various strategies to enhance the efficiency of its output. However, these methods have drawbacks such as increased preparation costs of TENG and additional mechanical losses. Additionally, the durability and sustained output capability of TENG triboelectric materials still pose unresolved issues in wearable sensors. Therefore, the focus of researchers' future research is to optimize the performance of TENG further while ensuring its other advantages, in order to improve self-powered wearable sensing devices.

## 2.2 Piezoelectric effect

The piezoelectric and piezoresistive effects transfer the strain force into electrical signals (Fig. 2(b)). They are both used in pressure sensors that can monitor local dynamic pressure changes.<sup>80</sup> But the piezoelectric effect performs well for power supply and forms the PENG system. The first PENG was proposed by Wang<sup>18</sup> in 2006. Then, for the application in wearable sensors, the PENG becomes popular.<sup>79</sup> In comparison with TENG, PENG can detect higher frequency motions with higher accuracy. Due to the small size, improving output performance remains a challenge that needs to be addressed. The material and structure are also the solutions for it.

The common piezoelectric materials involve piezoelectric ceramics,<sup>105</sup> piezoelectric crystals,<sup>106</sup> piezoelectric polymers,<sup>107</sup> and piezoelectric composite materials.<sup>108,109</sup> The modification of frictional materials focuses on surface effects, while the modification methods of piezoelectric materials mainly focus on bulk effects. These methods typically include ion doping,<sup>110</sup> phase structure modulation,<sup>111</sup> and multiphase coupling,<sup>112</sup> among others. Besides these, nanomaterials come into sight for their better performance in the morphology of nanowires (NWs) and nanosheets.<sup>113</sup> The first PENG is made of a zinc oxide nanowire array and has an output power density

of  $10^6 \mu\text{W m}^{-2}$ .<sup>18</sup> With continuous striving, the output performance of the nanowire PENG has been enhanced a lot. For instance, a PENG utilizing Mg-doped semi-insulating gallium nitride NWs can achieve an output power density of  $1.3 \times 10^8 \mu\text{W m}^{-2}$ , nearly a hundredfold increase.<sup>58</sup> And for nanosheets, a sulfur vacancy passivated monolayer molybdenum disulfide piezoelectric nanogenerator has a  $73 \mu\text{W m}^{-2}$  output power density. We have already made great progress in piezoelectric materials. However, due to the environmental stability and balance between performance and cost of piezoelectric materials, it is still necessary to improve the materials from multiple aspects to achieve higher heights and promote the development of PENG (Table 4).

In addition to the piezoelectric materials' performance, the structure of PENG is also essential. Inspired by the bionic shark gill, a biomimetic structure was designed to convert lateral elastic deformation into longitudinal elastic deformation when stretched. This characteristic successfully constructed a scalable multi-channel nanogenerator (Fig. 4(a)).<sup>44</sup> The device comprises two functional layers: the top layer, the main functional component, features multiple strip-shaped power generation units arranged in parallel. Every part has a sandwich structure of silicone resin, polyvinylidene difluoride (PVDF) metalized piezoelectric membrane, and polydimethylsiloxane (PDMS). The underlying layer serves as both support and friction, and it is made of silicone resin and silver NWs. The PDMS at the strip's base mimics gill arch cartilage for structural support, while the middle PVDF functions like gill filaments, crucial for energy conversion. Silicone on either side acts like gill muscles, connecting the unit to the base and adapting its shape during stretching. During operation, the strip units deform in unison, generating synchronous electrical responses. In addition to mimicking local animal structures, some PENGs are also designed to mimic plants. For example, a flower shape is applied (Fig. 4(b)). The flower shape is made of poly-L-lactic acid/barium titanate fiber, molybdenum electrode, and PCL films. We can easily see in Fig. 4(b) that the flower shape can gain more pressure stimulation sites to strengthen the output compared to the squared shape and the round shape.<sup>21</sup> In addition to biomimetic structures, increasing output sites is another effective method to enhance performance. An intelligent wristband system was developed using machine learning, featuring smart wristbands, multi-channel Bluetooth modules,

Table 4 Electrical properties of PENG of different sizes

Material	Dimension	Electrical properties
Polyvinyl alcohol <sup>114</sup>	0.404 cm <sup>2</sup>	0.927 V, 6 $\mu\text{A}$ , 340 $\mu\text{W m}^{-2}$
Expanded-PTFE <sup>78</sup>	0.75 cm <sup>2</sup>	1.4 V, 0.0035 $\mu\text{A}$ , 0.25 nC
BaTiO <sub>3</sub> <sup>59</sup>	1 cm <sup>2</sup>	0.29 V, 0.20 $\mu\text{A cm}^{-2}$ , 570 $\mu\text{W m}^{-2}$
PVDF <sup>35</sup>	4 cm <sup>2</sup>	56.5 V, 562 500 $\mu\text{W m}^{-2}$
Polycaprolactone/Ag <sup>57</sup>	4 cm <sup>2</sup>	30 V, 5.9 $\mu\text{A}$ ,
Ba <sub>0.85</sub> Ca <sub>0.15</sub> Zr <sub>0.10</sub> Ti <sub>0.90</sub> O <sub>3</sub> <sup>115</sup>	12 cm <sup>2</sup>	14.5 V, 28.5 $\mu\text{A}$ , 306.5 $\mu\text{W cm}^{-3}$
PVDF-TrFE/MXene <sup>116</sup>	12.56 cm <sup>2</sup>	42.3 V, 2 070 000 $\mu\text{W m}^{-2}$
PTFE <sup>117</sup>	14 cm <sup>2</sup>	150 V, 4.5 $\mu\text{A}$ , 240 nC
Ag/CuNRs/PDMS <sup>118</sup>	702.25 cm <sup>2</sup>	184 V, 203 $\mu\text{A}$ , 225 000 $\mu\text{W m}^{-2}$
PVDF <sup>119</sup>	26.88 cm <sup>3</sup>	0.41 V, 0.21 $\mu\text{A}$ , 45 nC

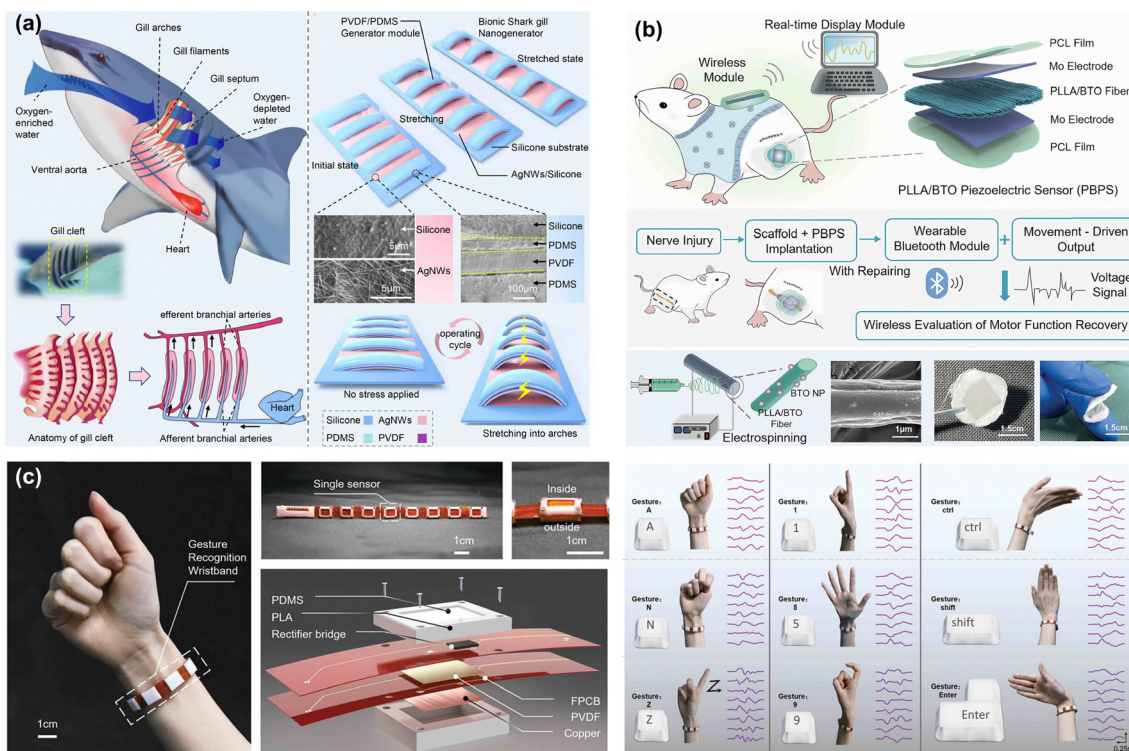


Fig. 4 Three cases of PENG application. (a) Bionic principle and structure of a bionic shark gill nanogenerator. Reproduced with permission from ref. 44. Copyright 2022 The Authors. Publishing Services by Elsevier B.V. on behalf of KeAi Communications Co. Ltd. (b) Schematic illustration of poly-L-lactic acid/barium titanate piezoelectric sensor structure and working diagram. Reproduced with permission from ref. 21. Copyright 2024 Wiley-VCH GmbH. (c) Physical image of gesture recognition wristband, schematic diagram of a sensor array, and schematic diagram of a single sensor. Output results of some representative gestures of letters, numbers, and commands. Reproduced with permission from ref. 46. Copyright 2022 Wiley-VCH GmbH.

and remote computer terminals (Fig. 4(c)).<sup>46</sup> Each wristband integrates a sensor array with eight sensors and a flexible printed circuit board (FPCB). A single sensor comprises a hybrid generator that combines TENG and PENG technologies, incorporating layers of PDMS, polylactic acid, PVDF, copper, metal, and two FPCB layers, which connect the sensors and act as circuit carriers. The researchers integrated two types of sensors into a small box measuring  $0.4\text{ cm} \times 0.8\text{ cm} \times 1\text{ cm}$ . TENG captures mechanical information from significant forces, while PENG focuses on light contact. The PENG operates on the principle that the fixed circumference of the wristband causes muscle and skin pressure on the sensor surface, leading to a deformation cycle: no deformation, slight deformation, maximum deformation, slight deformation, and back to no deformation. During fist movements, PENG yields a higher output. When a force of 5 N is applied by the wearer's skin to the sensor, the output of the hybrid generator is 1080 mV.

Currently, the significant advancements in the piezoelectric effect are making PENG increasingly prevalent. While these methods can greatly enhance the output performance of piezoelectric materials, their durability and stability still encounter challenges when it comes to integrating them into self-powered wearable sensors. This is due to their inherent sensitivity to temperature and humidity changes. Therefore, addressing these challenges is essential for fully harnessing the potential

of PENG in self-powered wearable sensing devices, marking a significant step forward.

### 2.3 Thermoelectric effect and pyroelectric effect

In addition to mechanical energy, the thermal energy of the human body presents another promising energy source for utilization. The thermoelectric effect is based on the potential difference caused by the migration of charge carriers (Fig. 2(c)),<sup>120</sup> while the pyroelectric effect is the potential difference and current caused by charge separation.<sup>121</sup> However, they are both widely utilized in self-powered technology.

Human skin can hinder heat dissipation, but thermoelectric devices (TEDs) can still gather enough energy from the body to power sensors that monitor human movements. To meet the demands of portable and real-time digital health devices, TEGs typically utilize organic thermoelectric materials that can conform to the human skin. TEDs are usually constructed by connecting multiple p-type and n-type thermoelectric materials in series and parallel.<sup>83</sup> Thermoelectric materials usually include organic thermoelectric materials, semiconductor thermoelectric materials, metal-based thermoelectric materials, and oxide-based thermoelectric materials. Besides the most commonly used organic materials, embedding inorganic rigid thermoelectric materials in silicone rubber is an effective approach for creating flexible thermoelectric devices. Han

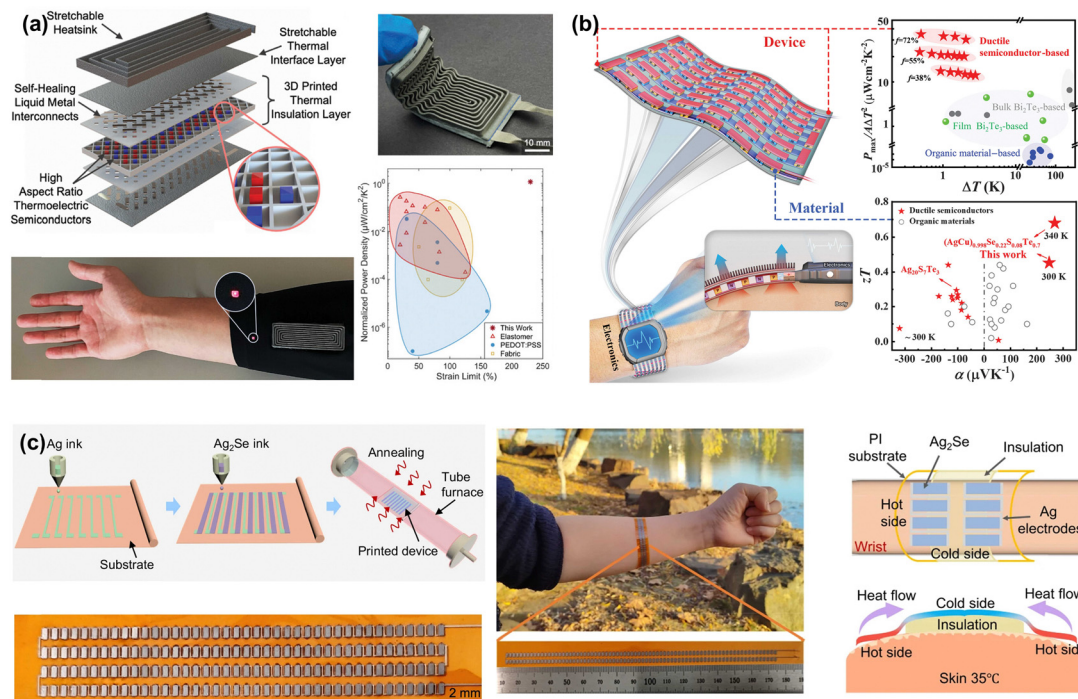


**Fig. 5** Three cases of TED application. (a) TED design and its multifunctional layer schematic and physical diagram. A scatter plot is used to compare soft and stretchable TED. Reproduced with permission from ref. 49. Copyright 2024 Wiley-VCH GmbH. (b) Schematic diagram of flexible thermoelectric devices for wearable electronic devices. The room temperature thermoelectric figure of merit ( $zT$ ) and Seebeck coefficient ( $\alpha$ ) of resilient inorganic materials and organic-based materials. Reproduced with permission from ref. 47. Copyright 2022, The American Association for the Advancement of Science. (c) Fabrication flow of a fully inkjet-printed  $\text{Ag}_2\text{Se}$ -based flexible device and the physical image worn on the wrist. Schematic diagram of thermoelectric power generation utilizing body heat. Reproduced with permission from ref. 122. Copyright 2024, The Author(s).

*et al.*<sup>49</sup> reported a 3D-printed soft architecture for damage-tolerant thermoelectric devices, setting a new performance record for energy harvesting while ensuring excellent consistency (Fig. 5(a)). This achievement is attributed to the successful integration of stretchable functional composite materials *via* 3D printing, the use of self-healing liquid metal interconnects, and the incorporation of inorganic thermoelectric materials within a thoughtfully designed device architecture. This combination optimizes thermoelectric energy conversion while maintaining structural integrity, addressing challenges related to stretchability, energy conversion efficiency, and durability during continuous use. In addition, conductive semiconductors are also driving the transformation of the potential of flexible thermoelectric materials. A series of high-performance p-type thermoelectric materials have been fabricated into thin, flexible  $\pi$ -shaped devices, achieving a power density of  $30 \mu\text{W cm}^{-2} \text{K}^{-2}$  (Fig. 5(b)).<sup>47</sup> Thermoelectric materials have undergone extensive optimization, significantly enhancing their output performance, but this has also increased costs. Fig. 4(c) illustrates the development of  $\text{Ag}_2\text{Se}$ -based thermoelectric thin films and flexible devices using inkjet printing. By manipulating ink formulations and adjusting printing parameters, large-area patterned arrays with micrometer-level resolution can be produced in a size-controlled manner.<sup>122</sup> The printed  $\text{Ag}_2\text{Se}$  thin films exhibit (001) texture characteristics, and excellent power factors are achieved through careful design

of the film composition and microstructure. This strategy underscores the potential to transform the design and manufacturing of multi-scale, complex flexible thermoelectric devices while also reducing costs.

Compared with TEG, PyNG has no external electric field limitation, making its performance easier to improve and more portable. However, due to the restriction of the pyroelectric coefficient, the output performance of PyNG did not significantly improve by simple structural design.<sup>123</sup> Crystallinity control and polymer modification have become the most effective ways to strengthen PyNG performance in practice. Moreover, Prestopino *et al.*<sup>20</sup> developed a layered double hydroxide (LDH) forming a new type of PyNG. The high gradient composition and energy levels of LDHs allow for easy adjustment of the size of the prepared devices. Two types of nanogenerators were designed using ZnAl LDH or MgAl LDH nanosheets, both exhibiting equivalent pyroelectric coefficients that can reach up to  $150 \mu\text{C K}^{-1} \text{m}^{-2}$ , or as low as  $-160 \mu\text{C K}^{-1} \text{m}^{-2}$ , which means the new type PyNG has a good performance. Although PyNG has efficient energy conversion, achieving self-powered capabilities, balancing performance improvement, and reducing costs remain goals for future development.

Utilizing thermoelectric and pyroelectric effects in self-powered technology allows for more efficient harnessing of human energy. Thermoelectric conversion is expected to

impact environmental protection and intelligent systems greatly. Future advancements will enhance performance, lower costs, broaden application areas, and integrate with other emerging technologies to advance sustainable energy development.

## 2.4 Other power supply modes

Recently, significant progress has been made in the area of self-powered wearable sensors. This progress has been driven by the development of various technologies such as nanogenerators which are the leading, biofuel cells (BFCs),<sup>84–86,124</sup> magnetoelectricity,<sup>64</sup> and other innovative power supply methods. All power supply methods have contributed to the development of wearable devices to varying degrees, making them more efficient and sustainable. In the previous text, we have

provided a detailed introduction to nanogenerators. There are many other power supply modes, and here we mainly describe two methods: BFCs, which generate electricity from organic compounds,<sup>84</sup> and magnetoelectricity, which harnesses the power of magnetic fields to produce electric current.

Generally speaking, BFCs use organic fuels and directly or indirectly utilize enzymes as catalysts to generate electricity (Fig. 2(d)).<sup>124</sup> However, their performance is limited by challenges such as inadequate enzyme immobilization and restricted electron transfer within the enzyme electrode.<sup>125</sup> The simplest approach is to combine BFCs with other power supply methods. Fig. 6(a) shows a system utilizing a self-voltage-regulated wearable microgrid for collecting and storing bioenergy from sweat.<sup>51</sup> This microgrid integrates enzyme biofuel cells and AgCl/Zn cells. It constantly delivers sweat to



**Fig. 6** The application cases of BFCs and magnetoelectric effect. (a) Schematic illustration of a fingertip-wearable microgrid system and its working principle, and optical image. Reproduced with permission from ref. 51. Copyright 2024, The Author(s), under exclusive license to Springer Nature Limited. (b) Schematic illustration of the metal hydrogel-based integrated w-BFC for sweat collection, energy harvesting, and self-powered sensor. Reproduced with permission from ref. 52. Copyright 2024 Wiley-VCH GmbH. (c) The process of preparing magnetic fabric. Microcomputerized tomography images of NdFeB magnetic yarn. A piece of  $1 \times 3 \text{ m}^2$  plain weave fabric formed by industrial weaving machines. Physical photograph and magnetic field distribution of  $5 \times 30 \text{ cm}^2$  magnetic fabric with good flexibility and foldable softness. Reproduced with permission from ref. 127. Copyright 2021 Wiley-VCH GmbH.

the sensors for the detection of multiple metabolites, while low-power electronic devices are used for signal acquisition and wireless data transmission. This wearable system operates entirely on fingertip sweat, enabling the detection of various physiological signals. Discovering new catalytic materials is another effective approach to improving the output performance of BFCs. The metal hydrogel-based sweat wearable BFCs have demonstrated high output and excellent stability, directly extracting energy from human sweat while sensing epidermal biomarkers with a self-sustaining power supply (Fig. 6(b)).<sup>52</sup> This highly porous and flexible metal hydrogel exhibits superior electrocatalytic capabilities, oxidizing ascorbic acid and sweat metabolites at the anode, and reducing O<sub>2</sub> at the cathode. The future prospects of biofuel cells are very broad. With the continuous advancement of technology, their efficiency and stability will be further improved, and their application fields will also continue to expand.<sup>126</sup>

In addition to BFCs, some researchers have turned their attention to magnetoelectric effects, usually utilized in large generators. Usually, only one coil and magnet are needed to achieve a power supply. When we wrap a flexible magnet in a copper coil covered by an Ecoflex sleeve and attach it to a finger, it can transfer physiological energy related to finger motions into electrical energy (Fig. 6(a)).<sup>64</sup> This setup allows for real-time gesture interaction, enabling long-distance control of robot hands and vehicles utilizing human hands. Additionally, some smart fabrics utilize magnetic electric power supplies. A scalable flexible magneto-electric clothing generator can generate electricity through arm movements (Fig. 6(c)).<sup>127</sup> The particle flow spinning approach enables the production of continuous magnetic yarns and fabrics using industrial looms, allowing for large-scale manufacturing at lower costs. The integration of magnetic fabrics and conductive wires on both sides of the armpit generates a continuous and stable voltage and current as the arm swings. Moreover, these magnetic fabrics can operate underwater without the need for sealing and are effective in both acidic and alkaline environments, as well as extreme temperatures. For their high energy transfer efficiency and output power density, magnetoelectric energy is often combined with other power supply modes to create a hybrid generator, which can power multifunctional wearable sensors.

With the continuous advancement of techniques, power supply methods for wearable sensors have evolved to encompass a variety of approaches. While some methods may be used less frequently, they have undergone significant development and are now applicable to a broad scope of scenarios in powering wearable sensors. These diverse power supply methods are essential for advancing and innovating wearable sensor technologies.

## 2.5 Hybrid power supply mode

Given the advantages and disadvantages of various power supply methods, researchers have learned from each other's strengths and weaknesses and developed a new research direction-hybrid power supply mode. There are two main

directions: one is to combine different nanogenerators for use, and the other is to combine nanogenerators with other power supply modes.

By integrating multiple nanogenerators, wearable devices can increase their power output and expand their application range while ensuring device miniaturization. This combination of various nanogenerators has greatly advanced the development of self-powered wearable sensors, creating new opportunities for innovative and efficient designs. TENGs and PENGs are commonly used power generation devices in self-powered wearable sensors and hybrid nanogenerators (HNGs). One way is to find a material that is capable of serving as both piezoelectric and triboelectric materials. In Fig. 7(a), an energy harvester and sensing patch (EHSP) was designed consisting of multiple layers, with a composite layer sandwiched between a flexible mesh electrode and an elastic/thermochromic dye layer.<sup>128</sup> The bottom electrode is first layered with the potassium niobate composite film and covered with an elastic material, and a thermochromic dye is loaded in the elastic material. The elastomer carries a negative charge and therefore acts as a negative frictional dielectric in TENG, HNG, and EHSP structures. It is used as a sensor and energy harvester. The EHSP can be mounted on the human body and extended to other daily applications. Another method is to splice or stack piezoelectric materials and triboelectric materials together. The simplest way of splicing is for each component to occupy half, and when the device vibrates and rubs with the movement of the body, HNGs begin to collect energy. In one example, the energy collected was most likely sufficient to support low-level vagus nerve stimulation for treating atrial fibrillation,<sup>39</sup> while stacking multiple triboelectric and piezoelectric materials can achieve multiple power generations through a single vibration.<sup>129</sup> In addition to the combination of TENGs and PENGs, other nanogenerators also have different combinations of power supply, such as PENGs and PyNGs.<sup>118</sup> With the deepening of research, the power supply capability of HNGs continues to enhance, increasing their ability to capture human energy and expanding their applications in various fields.

Another approach is to combine nanogenerators with other power modes. They collect different types of energy from the environment while collecting human energy to improve the output capacity of the generator. In addition to common sources such as solar<sup>130</sup> and wind energy, radiofrequency energy is also gradually gaining attention from people (Fig. 7(b)). Thus, a hybrid energy harvester that combines radio frequency and triboelectric energy was designed.<sup>43</sup> The hybrid energy harvester system comprises a wearable rectifier antenna, a TENG, and a power management circuit. Researchers have proposed a standardized fabric circuit board that utilizes quasi-surface mount technology, which integrates modules on the fabric architecture. The multifunctional fabric constructed in this way can improve the controllability of the collected mixed energy while enhancing the mechanical robustness of the system. Electromagnetic generators are commonly used as a power supply method for large generators due to their advantages in continuous power output and efficiency.

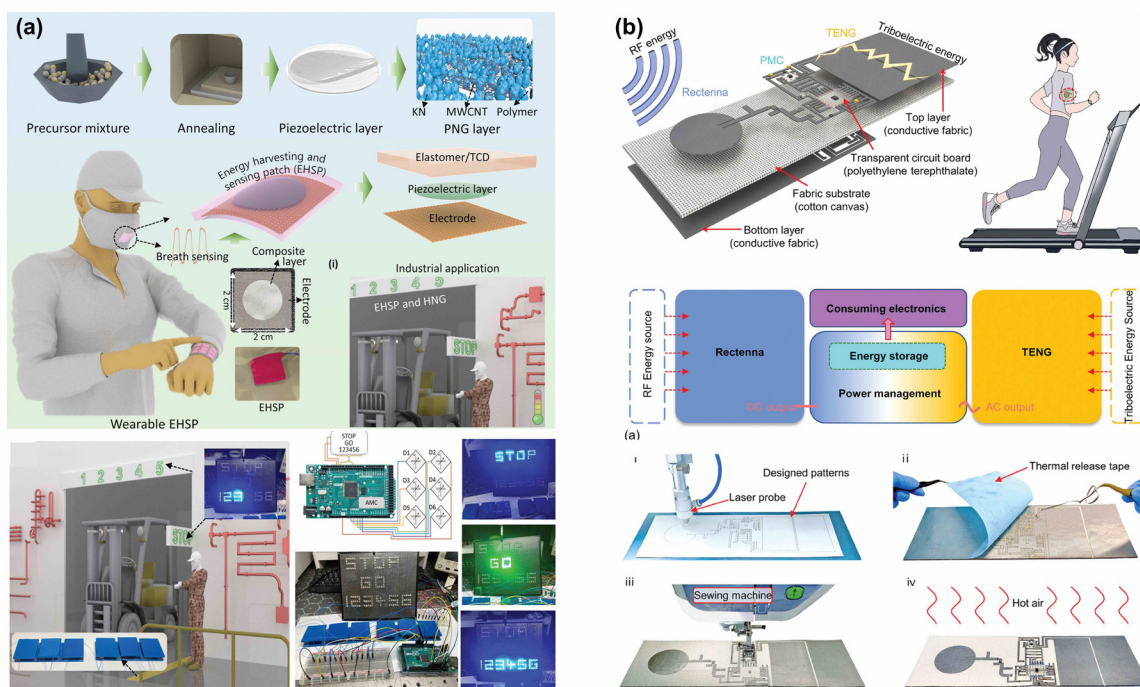


**Fig. 7** Hybrid power supply mode. (a) The preparation, schematic diagram, photographic images, and various applications as a wearable device. PENG, TENG, and EHSP device structures are used to optimize electrical output and thermochromic properties. Working mechanism of the EHSP. Reproduced with permission from ref. 128. Copyright 2024 The Author(s). *Advanced Functional Materials* published by Wiley-VCH GmbH. (b) Preparation, schematic diagrams, photographic images, and industrial applications of EHSP. Reproduced with permission from ref. 43. Copyright 2024 The Authors. *Advanced Science* published by Wiley-VCH GmbH.

Electromagnetic generators and TENGs are often used together because electrostatic induction and electromagnetic induction are two non-contact effects with minimal mutual interference.<sup>88</sup> A highly coupled triboelectric–electromagnetic magnetic-levitation hybrid nanogenerator was designed. During TENG's contact separation process, the magnetic flux in the electromagnetic generator coil creates a voltage between the coil and the Cu electrode. The unique design of the magnetic-levitation hybrid nanogenerator adopts a shared coil electrode configuration, which enhances coupling without increasing additional volume.

Due to the intermittency and instability of most self-powered technologies, energy storage devices have become essential components in flexible and wearable electronic systems.<sup>126</sup> Among various energy storage solutions, fabric batteries have emerged as a promising option for self-powered wearable devices.<sup>65,131–133</sup> Fabric batteries combine battery technology with flexible materials for use in wearable devices, flexible electronics, and smart textiles.<sup>134</sup> By using conductive fibers and materials, these batteries are soft, stretchable, and comfortable to wear like regular fabric.<sup>135</sup> Here's an example. Jiang *et al.*<sup>131</sup> developed a fiber electrode with a channel structure for high-performance flexible batteries. They used a polymer gel electrolyte instead of a traditional liquid electrolyte to enhance safety and flexibility. By rotating electrode fibers to create organized channels and incorporating small and large holes on the surface, they improved the penetration of the gel electrolyte, ensuring a

stable interface. This design boosts the battery's energy density to about  $128 \text{ Wh kg}^{-1}$  and demonstrates excellent electrochemical performance and long-term stability. With the ongoing advancement of technology, fabric batteries are anticipated to be widely utilized in areas such as smart textiles, wearable devices, and healthcare, providing greater convenience and innovation to daily life.<sup>136</sup>

The hybrid power supply method extends the operation time of self-powered wearable sensing devices, enhances energy efficiency, improves device autonomy and reliability, and reduces battery dependency. However, this also increases the complexity of system design, necessitating precise power management techniques and stable energy storage methods. Overall, hybrid power sources boost the durability and environmental sustainability of wearable devices while enhancing their long-term reliability, providing greater convenience and surprises in daily life.

### 3. Different wearing styles

With the continuous advancement of technology, people's demand for improved medical standards is also increasing. People hope to always protect their health in their daily lives.<sup>137</sup> The increasing demand has led to the rapid popularization of health monitoring, exercise tracking, and smart devices, which has accelerated the development of lightweight, portable, and self-powered wearable sensors.<sup>138</sup> It is expected that further integration of technologies such as AI and big data to achieve

more intelligent functions, and the application scope will continue to expand. Whether in health monitoring, environmental protection, or personalized fashion, self-powered wearable sensing devices have the potential to change our way of life.<sup>7</sup> These sensors have thus spawned various wearing methods to meet different application scenarios, such as using smart fabrics, flexible devices, and exoskeletons.

The following section will offer a comprehensive overview, detailing each wearing method's development and specific application scenarios.

### 3.1 Smart fabrics

The development of smart fabrics dates back to the 1980s, with early research mainly focused on integrating sensors and electronic components into traditional fabrics.<sup>139</sup> With the advancement of technology, particularly in materials science and textile engineering, smart fabrics have evolved into multifunctional textiles capable of sensing the environment, transmitting information, and interfacing with other devices. Combining self-powered wearable sensors with smart fabrics, which we call self-powered smart fabrics, has also made progress in portability and customization.<sup>140</sup> But problems related to flexibility, breathability and integration with clothing still need to be addressed.<sup>141</sup>

The weaving process of smart fabrics has higher complexity compared to traditional textiles, as it not only requires the basic functions of textiles to be implemented, but also integrates sensors, circuits, conductive materials, *etc.* to achieve intelligent interaction, data acquisition, or energy transmission functions.<sup>142,143</sup> The integration of intelligent fibers with traditional textile machines is mainly achieved through material and process adaptation, structural design optimization, and innovation in large-scale production.<sup>144</sup> In terms of integration, conductive fibers, such as carbon fibers,<sup>145</sup> conductive polymers,<sup>146–148</sup> and metal fibers<sup>149</sup> are used to achieve electronic functions. These conductive fibers can be blended with ordinary fibers or woven separately into fabrics, forming the basic components of circuits. For example, electrospun temperature sensors made from PVDF/LiCl nanofibers can balance the flexibility and breathability of textiles while also reducing the energy consumption of portable electronic devices.<sup>150</sup> Coaxial coating, interlacing, and twisting are three typical strategies for assembling fiber electrodes into fiber devices.<sup>151</sup> The coiled structure fibers manufactured using melt spinning technology and twisted insertion can withstand up to 100% axial tension, achieving a high energy density of  $80 \text{ mJ cm}^{-2}$ .<sup>152</sup> The common weaving methods include plain weave, twill weave, and satin weave, and the specific choice depends on the flexibility, conductivity, and intended use of the fabric. In textile processing, smart fibers and conductive yarns are intricately woven into embedded electrode structures using three-axis looms or industrial knitting machines.<sup>142</sup> In addition, combined with the melt spinning process, a high energy output of  $87 \mu\text{W cm}^{-3}$  has been achieved.<sup>153</sup> Furthermore, smart fabrics often incorporate additional components like sensors, LED displays, heating elements, and energy harvesters, which are integrated

through techniques such as direct embedding and fabric circuit design. In essence, the creation of smart fabrics represents a convergence of traditional textile craftsmanship with cutting-edge interdisciplinary technologies in electronics and sensing, enabling the development of innovative and multifunctional wearable solutions. Large-scale production is facilitated by a continuous spinning and weaving process, combined with cost-effective pre-mixed masterbatch technology, ensuring seamless integration with existing production lines.<sup>153</sup> This approach offers an efficient and affordable solution for the commercial application of electronic textiles.

The development of self-powered smart fabrics was first considered to solve the problems of comfort and breathability. Fig. 8(a) showcases a high-integration and high-recognition system that consists of a self-powered multi-point body motion sensing network (SMN) building on a fully woven structure.<sup>154</sup> The SMN is developed through traditional knitting and innovative digital embroidery techniques. It can detect dynamic parameters such as limb movements and coordination during walking and convert them into electrical signals. This SMN exhibits excellent pressure sensitivity and a rapid response time, all while ensuring outstanding breathability, moisture permeability, washability, and high stability. While addressing these issues, we have started to explore further functionalization of self-powered smart fabrics and their potential applications in daily life and high-risk work scenarios. In daily life, the most common use of self-powered smart fabrics is to monitor human movement and physiological conditions. Just like the smart fabric powered by TENG as shown in Fig. 8(a), it can be used for gait recognition. In addition, integrating thermoelectric devices for collecting human thermal energy into self-powered smart fabrics can enable continuous monitoring of health status anytime and anywhere. A stretchable MXene-based thermoelectric fabric harnesses body heat by utilizing the temperature difference with the environment, converts it into electrical energy, tracks breathing rates, and monitors joint states through deformation.<sup>141</sup> At the same time, it can collect thermal energy from the environment for more stable detection. In addition to motion monitoring, self-powered smart fabrics are often used for functions such as intelligent monitoring<sup>155</sup> and intelligent human-machine interaction.<sup>101</sup> The requirements for home intelligent monitoring devices include easy concealment, simple operation, and mobile monitoring. Mechanical luminescent TENG fibers (MLTENGf) constructed based on lightweight carbon nanotube fibers ensure good stretchability while self-powered (Fig. 8(b)).<sup>155</sup> The carefully designed MLTENGf delivers a remarkable 200% increase in electrical signals and distinct optical signals, both on land and underwater, by utilizing its mechanoluminescent-triboelectric synergistic effect. As a carpet, the MLTENGf generates a signal when a stranger steps on it, activating an alarm that produces a green light, which is then wirelessly conveyed to a mobile phone *via* Bluetooth. The nanofibers can also be used for underwater communication. If it can be applied underwater, it is easy to associate it with application scenarios like high-risk fire scenes. Fig. 8(c) depicts a multifunctional



**Fig. 8** Smart fabrics. (a) Structural design of a textile-based SMN and schematic diagram of a highly integrated gait recognition system. Schematic diagram of the manufacturing process and parameters of Ag-PE core-sheath composite yarn. Atomic-scale-electron-cloud potential-well model to describe the contact electrification between conductive fabric and PE sheath yarn. Reproduced with permission from ref. 154. Copyright 2023 Wiley-VCH GmbH. (b) Schematic diagram and SEM image of MLTENG principle. Photos of stretchable MLTENG and their corresponding optical images and dynamic loading structure diagrams. Output voltage of MLTENG at different distances and its application and transmission in water. Reproduced with permission from ref. 155. Copyright 2024 The Author(s). Advanced Science published by Wiley-VCH GmbH. (c) Illustration of the synthetic route of conductive fabric/polyphthalamide. Application of fire alarm system based on thermoelectric effect and TENGs. Reproduced with permission from ref. 156. Copyright 2024 Elsevier B.V. All rights are reserved, including those for text and data mining, AI training, and similar technologies.

intelligent textile that serves as a dual fire warning system.<sup>156</sup> It incorporates thermoelectric performance, TENG, flame retardancy, and hydrophobic functionality into a unified system. The flame retardant mechanism combines principles of condensed-phase and gas-phase flame retardancy. In the event of a fire or personal activation of alarm devices, the microcontroller chip promptly sends a distress signal to a mobile phone to ensure an effective alarm. Due to the wide applicability of self-powered smart fabrics in daily life, reducing their cost has also become one of our priorities.<sup>157</sup>

The future of self-powered smart fabrics will continue to advance despite impressive progress.<sup>140</sup> These fabrics will deepen in terms of multifunctionality, integration, and comfort, fully utilizing the latest advances in technology.<sup>158</sup> They will be able to adapt to various environments and application scenarios, from sports equipment to medical monitoring, and even daily wear, demonstrating greater flexibility and powerful

performance. As materials science and electronic technology continue to integrate, these fabrics are poised to transform our understanding and use of clothing entirely.<sup>159</sup>

### 3.2 Flexible devices

The development of flexible devices dates back to the late 20th century, initially focusing on basic research in flexible electronics and wearable technology.<sup>160</sup> Since the beginning of the 21st century, rapid technological advancements have led to a significant surge in demand for wearable devices. This trend not only encourages the widespread use of stretchable devices in health monitoring, such as heart rate tracking, motion detection, and sleep analysis, but also supports their integration in smart homes and the Internet of Things, including smart lighting control and environmental monitoring systems.<sup>161</sup>

In order to improve the performance, flexibility, and comfort of flexible devices, 3D printing and microelectromechanical

systems (MEMSs) play a crucial role in the manufacturing of self-powered wearable flexible devices. Both can provide high-precision, complex structures, and highly customized solutions. 3D printing brings significant advantages in complex structures and personalized customization. The key components of self-powered equipment, such as sensors, batteries, and energy harvesting modules, typically need to be highly customized according to application requirements. 3D printing allows for precise structural design at the micrometer level. In addition, self-powered wearable devices typically require a casing or support structure to protect electronic components and enhance the comfort and durability of the device. 3D printing can create customized flexible shells with high comfort and elasticity, which can adapt to the dynamic movement of the human body while providing sufficient protection. MEMSs have a wider range of applications in precision component manufacturing. MEMSs refer to the optimization design, processing, assembly, system integration, and application technology of sub-millimeter, micrometer, and nanometer-scale components, as well as components or systems composed of these components. MEMSs can manufacture high-precision flexible circuit boards and create microcircuits on flexible substrates through etching technology. This circuit can achieve high-density integration and has excellent flexibility and bendability, making it suitable for wearable devices that come into contact with the skin. In addition, MEMSs can be used to manufacture high-energy density micro batteries or supercapacitors, providing sufficient power support for self-powered wearable devices. In the manufacturing of self-powered wearable flexible devices, 3D printing and micro–nano processing technologies are often combined to leverage their advantages.

At present, flexible devices have achieved high performance and integration, and they are developing towards intelligence and self-powered, enabling devices to work independently without external power sources. This innovation greatly enhances the flexibility and convenience of the equipment.<sup>162</sup> Self-powered flexible devices are available as adhesive patches, which allow users to attach them to their skin easily. Nonadhesive patches usually use straps and tape assistance to adapt to different usage scenarios and needs.

**3.2.1 Adhesive patches.** Adhesive patches are designed to be lightweight and easy to wear, so patients feel a minimal burden in their daily lives. The materials for these patches are carefully selected to minimize skin irritation and are suitable for long-term use, especially in situations that require continuous monitoring or treatment. Patients can maintain natural movement while wearing the patch, without feeling uncomfortable or impacting their daily life.<sup>163</sup>

Modern adhesive patches are integrated with advanced sensor technology, allowing real-time monitoring of vital signs.<sup>164,165</sup> While combined with AI, this technology creates more precise and flexible human–machine interfaces.<sup>166,167</sup> The first problem that adhesive patches need to solve is how to better adhere to the human body. In Fig. 9(a), a solid-state frictional electric patch is shown, which uses a composite material called polyethylene oxide/waterborne

polyurethane/phytic acid to form an effective current collector, along with silicone rubber as the friction layer.<sup>164</sup> Autonomously adhering to non-flat skin or clothing surfaces, this patch serves as a tactile sensor or skin input touchpad for detecting physiological motions and enabling remote control of electrical appliances. Combining scalability, stretchability, and transparency, it meets a diverse array of application needs, from transparent electronics to artificial skin and intelligent interfaces. One of the key factors of these devices is the hydrogel electrolyte. In one example, a conductive double mesh ionic organic hydrogel with antifreeze, self-healing, adhesion, and toughness was constructed.<sup>167</sup> Utilizing high-performance ionic organic hydrogel as the key material for body motion strain sensors and all-solid-state supercapacitors enables the creation of self-powered strain sensors and flexible supercapacitor systems. In addition to the adhesive patches composed of hydrogels, polycationic modified carbon nanodots/polyvinyl alcohol nanocomposite polymer electrolytes were utilized as the primary triboelectric materials to build an innovative type of nanocomposite polymer electrolyte-based fiber TENGs, which expanded the material limitations of electronic skin.<sup>166</sup>

With the continuous advancement of technology, these patches are becoming more functional and personalized in design. Manufacturers can customize patches that suit the specific needs of different patients and provide tailored medical solutions. This personalized medical service improves patient compliance and enhances treatment effectiveness, allowing every patient to have a more intimate and effective nursing experience. Adhesive patches play an increasingly important role in modern medicine, providing convenience and protection for patients' health management.

**3.2.2 Straps and tape-assisted nonadhesive patches.** Due to the inability of nonadhesive patches to autonomously adhere to the human body, straps or adhesive tapes are usually used for assistance.

In addition to the nonadhesive patches assisted by straps used for monitoring heartbeat and pulse rate and other physiological activities mentioned earlier, nonadhesive patches assisted by straps can also be used for detecting various secretions produced by the human body, such as sweat detection. Just like Fig. 9(b) shows, a wireless wearable sweat analysis device can continuously and *in situ* monitor biomarkers at the molecular level while effectively converting the mechanical energy of human movement into electrical energy.<sup>89</sup> And it can wirelessly transmit sensor data to the user interface through bluetooth. In addition to the fluids secreted by the human body, gases are also one of the standards for detecting human health. Since COVID-19, masks used to detect or inhibit the spread of pathogens have made great progress.<sup>169</sup> Nonadhesive patches for detecting harmful gases are important for maintaining human health. For instance, a self-powered and reusable all-in-one NO<sub>2</sub> sensor has been proposed.<sup>170</sup> This sensor is structurally and functionally coupled to the battery, providing ultrahigh sensitivity, linearity, an ultralow theoretical detection limit, and humidity immunity. Moreover, it can be used as wearable electronics to provide early and remote

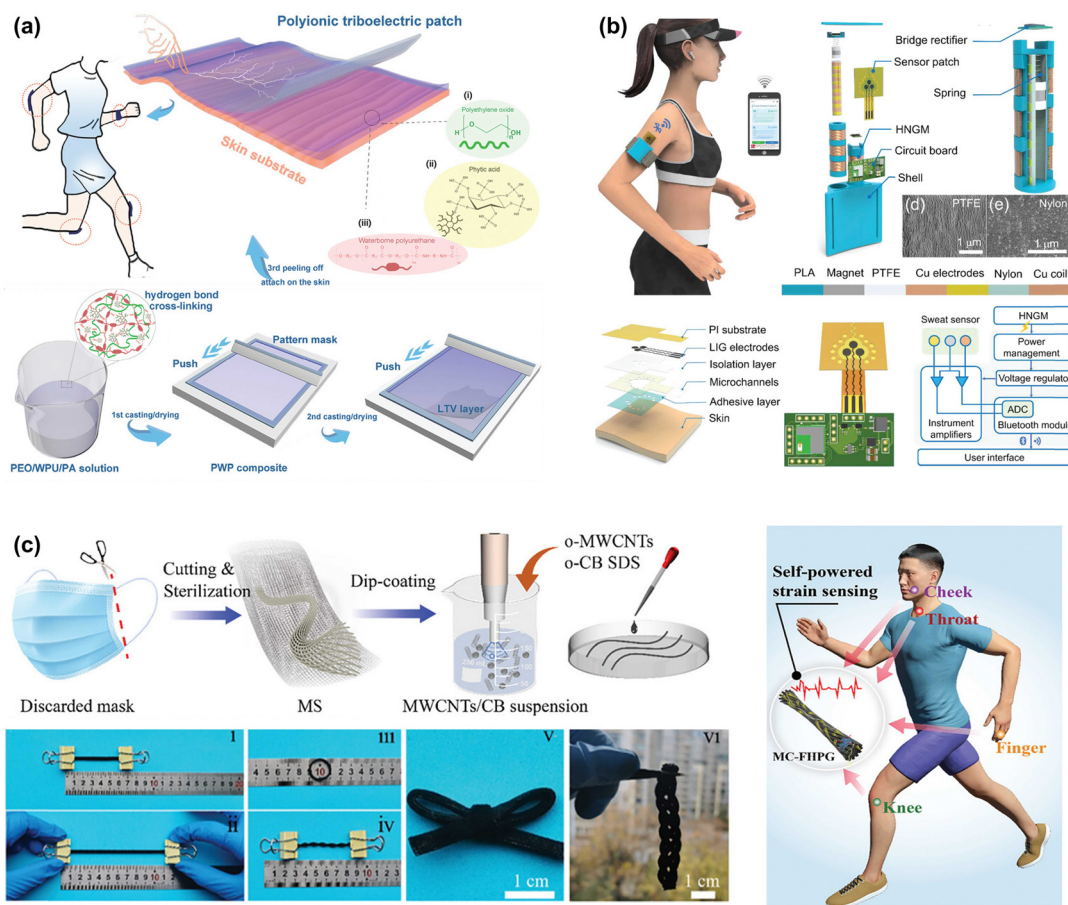


**Fig. 9** Three cases of flexible devices. (a) Schematic illustration for the preparation of polyionic triboelectric patch. The patch structure consists of a polyethylene oxide/waterborne polyurethane/phytic acid current collector and silicon rubber tribolayer. Reproduced with permission from ref. 164. Copyright 2021 Wiley-VCH GmbH. (b) Schematics and structure diagram of the self-powered SWSAS for wireless molecular monitoring. Structural design of the HNGM. The SEM images of the etched PTFE and nylon film surface. Structure diagram of the sweat sensor patch. Reproduced with permission from ref. 89. Copyright 2022 Wiley-VCH GmbH. (c) Schematic illustration of the fabrication process for MC-FHPG. The stretchability, flexibility, and knittability of the MC-FHPG. Self-powered wearable strain sensing performance and human behavior monitoring applications. Reproduced with permission from ref. 168. Copyright 2023 Wiley-VCH GmbH.

warning of gas leakage. Although nonadhesive patches assisted by straps can adhere to the human body, they cannot fit the curves of the body well.

Therefore, some nonadhesive patches use various non-toxic adhesive tapes to adhere to the human body without affecting their performance. For environmental considerations, a stretchable hydro photovoltaic power generator based on fiber optics has been designed, which has the advantages of high output, portability, repeatability, and sustainable power generation (Fig. 9(c)).<sup>168</sup> COVID-19 has countless discarded masks. The hydro photovoltaic power generator is a functional micro/nano water diffusion channel based on discarded mask strips and oxidized carbon nanomaterials, enabling the applied water to generate power continuously in the process of spontaneous flow and diffusion. In addition to the water vapor evaporated by the human body, the heat it emits is also a significant energy source. A self-powered, ultra-sensitive strain sensor is designed based on a graphene thermoelectric composite thread using a simple 3D extrusion method.<sup>82</sup> High-sensitivity strain and temperature detection can be achieved through the current

generated by the thermoelectric effect. Adhesive tape-assisted nonstick patches have various applications in daily life, which will not be elaborated on here.

With the continuous advancement of technology and the expansion of their application scope, flexible devices have shown broad application prospects. They are anticipated to play a greater role in various fields such as healthcare, sports, fashion, *etc.* in the future, changing our way of life and health management.

## 4. The digital health application of self-powered wearable sensors

Digital health is an evolving field that encompasses the extensive use of digital technology in healthcare and health management.<sup>171</sup> These technologies include health monitoring devices, mobile health applications, electronic health records, remote healthcare, AI, and data analysis. The core goal of digital health is to improve the efficiency, accessibility, and

personalization of medical services while helping individuals better manage their health and make wiser life choices.<sup>172</sup>

In this context, the real-time, portable, and remote communication capabilities of self-powered wearable sensors make them highly applicable in various digital health environments. These sensors can continuously monitor users' health status and transmit data in real-time through smartphones or other devices, helping users and healthcare providers stay informed about health information at all times. This feature not only improves the accessibility of data but also provides a foundation for the development of personalized medical plans.

In this section, the application of self-powered wearable sensors in digital health is mainly introduced. These applications can be categorized into proactive prevention, intelligent diagnosis, precision treatment, and scientific rehabilitation.

#### 4.1 Proactive prevention

Proactive prevention is a health management and risk control strategy focusing on taking proactive measures to reduce the likelihood or impact of future problems or diseases.<sup>174</sup> This approach includes early intervention, health education, regular health monitoring, lifestyle adjustments, and risk assessment to identify potential health risks. By using self-powered wearable sensors and remote communication control programs, it is

possible to track users' health data, detect abnormal situations, and take real-time preventive measures.<sup>175</sup> This data-driven approach aims to improve health awareness, promote active health management, and ultimately reduce the overall incidence rate of chronic diseases while improving the quality of life.<sup>176</sup>

Since the onset of COVID-19, there has been remarkable progress in the development of masks designed to detect exhaled gases.<sup>169</sup> On the mask, there are often exhaled breath condensates (EBCs) formed by the condensation of water vapor in the exhaled gases from the human body. EBCs contain a wealth of physiological information about individuals. As a result, a mask-based system called exhaled breath conditioned analysis and respiratory evaluation (EBCare) is created for monitoring EBC biomarkers (see Fig. 10(a)).<sup>173</sup> EBCare can continuously monitor EBC analytes during indoor and outdoor activities. EBCare has been validated for evaluating metabolic status and respiratory inflammation both in healthy individuals and in patients with related diseases. Additionally, preventing wound infections is also a major aspect of proactive prevention. A wearable self-powered wound dressing, shown in Fig. 10(b), can be sensitized by different inducements from the human body and offers on-demand treatment for both normal and infected wounds.<sup>96</sup> The height-adjustable dressing consists

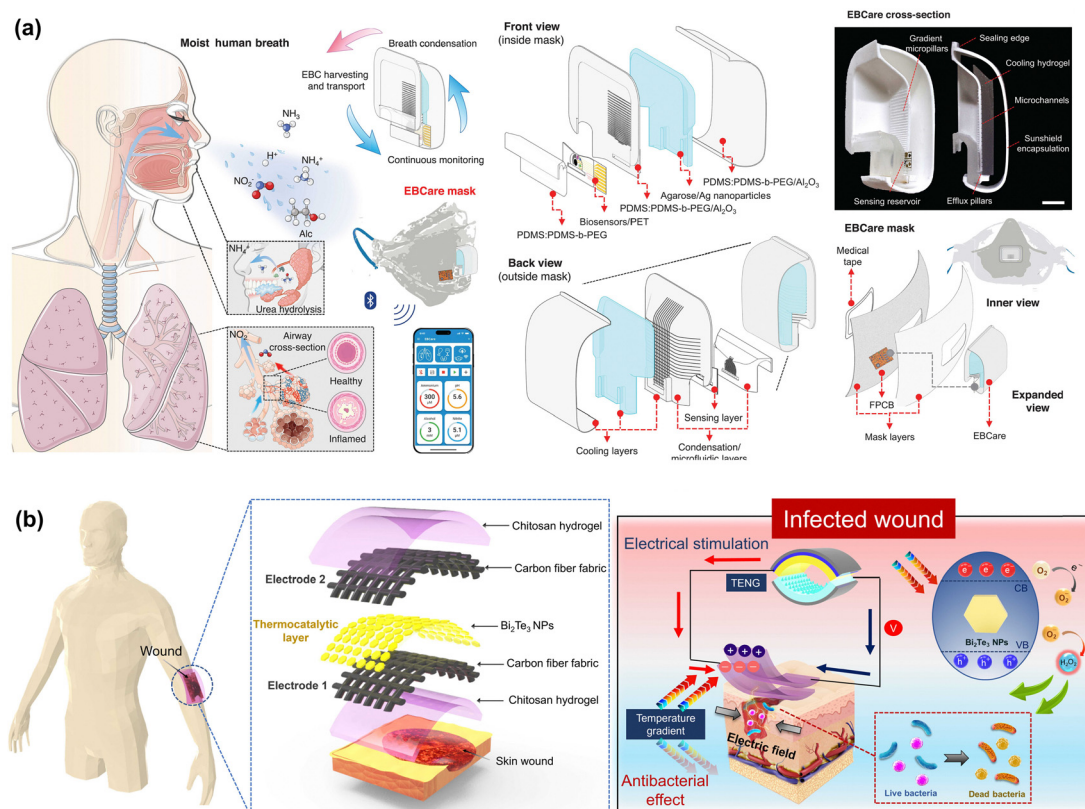


**Fig. 10** Proactive prevention. (a) Smart EBCare mask for efficient harvesting and continuous analysis of exhaled breath condensate. Schematic showing the expanded and inner views of the smart mask integrated with an EBCare device. Reproduced with permission from ref. 173. Copyright 2024, The American Association for the Advancement of Science. (b) Structural design of the wound dressing with  $\text{Bi}_2\text{Te}_3$  NPs as the thermocatalytic layer, chitosan hydrogel as the encapsulation layer, and chitosan-coated carbon fiber fabric as the electrodes. Mechanism of the wound dressing for healing normal and infected wounds. Reproduced with permission from ref. 96. Copyright 2023, The American Association for the Advancement of Science.

of thermally catalyzed bismuth telluride nanoplates ( $\text{Bi}_2\text{Te}_3$  NP) based on a carbon fiber fabric electrode. It is activated by the surrounding temperature difference to produce hydrogen peroxide in a controllable manner, effectively inhibiting bacterial growth. This self-powered dressing has the potential to facilitate personalized wound care, leading to enhanced healing outcomes. In addition to preventing infections and infectious diseases, researchers also aim to actively prevent other diseases. The principle involves isolating or killing potential pathogens, which will not be elaborated on here.

In the future, these self-powered wearable sensors, combined with AI and big data analysis, will provide personalized prevention recommendations and help users develop health plans that are suitable for themselves. These devices will also be more lightweight, comfortable, and have longer battery life, thereby enhancing the wearing experience. In addition, real-time data sharing with healthcare providers will enable doctors to obtain patients' health information promptly, thereby making more accurate decisions. Ultimately, these technologies will better support remote healthcare services, allowing users to receive guidance from doctors at home, promoting convenience and accessibility for proactive prevention, and improving overall health levels.

#### 4.2 Intelligent diagnosis

Intelligent diagnosis utilizes advanced techniques such as AI, machine learning, and data analysis to support or partially replace traditional medical diagnostic processes.<sup>177</sup> This innovative method helps healthcare professionals identify diseases and health issues faster and more accurately by analyzing large amounts of health data, imaging data, and patient history information. Combined with self-powered wearable devices, innovation in remote healthcare can also be achieved. Medical professionals can remotely access users' health data, provide timely feedback and guidance through intelligent diagnostic systems, avoid unnecessary waiting for medical treatment, and improve the accessibility of medical services.<sup>178</sup>

One of the primary goals of intelligent diagnosis is to assist doctors in accurately diagnosing patients' diseases. The stethoscope is the most commonly used diagnostic equipment by doctors, which is why a digital stethoscope was developed. Fig. 11(a) illustrates a wireless, sustained soft wearable stethoscope (SWS) used to quantitatively diagnose a range of diseases.<sup>179</sup> This software device enables the monitoring of consecutive cardiopulmonary sounds with minimal noise and classification signal anomalies, effectively addressing the shortcomings of current digital stethoscopes, which are often too bulky for consecutive auscultation. In addition to medical devices, developing various testing equipment is a key objective of intelligent diagnosis. A flexible sensor for multimodal muscle state monitoring has been designed by integrating a snake-shaped surface electromyography electrode with a fingerprint force electromyography sensor into a patch approximately 250  $\mu\text{m}$  thick (Fig. 11(b)).<sup>180</sup> This design allows for a comprehensive assessment of muscle condition while maintaining a compact form. It ensures the stability of fingerprint force

electromyography sensors during mechanical deformation and vibration. By analyzing the time-domain and frequency-domain characteristics of electromechanical coupling signals, this patterned coupling sensing patch demonstrates practical applications in muscle strength tracking, fatigue assessment, and muscle dysfunction recognition. Remote medical diagnosis is also a significant area for the advancement of intelligent diagnosis. It has enhanced the efficiency and quality of medical services, as well as improved the treatment experience and quality of life for patients. Chen *et al.*<sup>181</sup> designed a wearable sweat detection platform that utilizes surface-enhanced Raman spectroscopy and is capable of visually and intelligently analyzing sweat. The platform is made of colorimetric paper containing silver NWs (AgNWs) (Fig. 11(c)).<sup>181</sup> By taking photos with a smartphone, the platform can intelligently quantify the pH value and volume of the sweat using image recognition technology. In diagnosing gout, the platform collects surface-enhanced Raman spectroscopy spectra of human sweat containing uric acid and analyzes them using AI algorithms. Furthermore, the integration of remote medical diagnosis and self-powered wearable sensors boosts patients' feelings of being actively involved. Patients can track their health status at any time using wearable devices and share feedback with their doctors, thereby actively engaging in health management. This interaction not only improves patients' awareness of their health but also reinforces their treatment adherence.

The combination of intelligent diagnosis and self-powered wearable sensors will advance with the development of AI. This will enable accurate health assessments and personalized treatment plans. The development of technology will reduce the cost of telemedicine and wearable devices, and improve access to high-quality medical services, especially in remote areas. A user-friendly interface will enhance the patient experience, encourage active health monitoring and management participation, and promote more efficient, intelligent, and personalized medical services.

#### 4.3 Precision treatment

Precision therapy emphasizes tailoring treatment plans based on multiple data points such as the patient's genomic information, lifestyle, and environmental factors.<sup>182</sup> Self-powered wearable sensors are essential to this process. The combination of precision treatment and self-powered wearable sensors brings new opportunities for personalized medicine. They can capture dynamically changing data and help doctors adjust treatment strategies promptly. For example, for patients with diabetes, monitoring blood glucose levels can help doctors respond quickly and adjust insulin dosage when necessary.<sup>183</sup> This combination enables doctors to develop more accurate treatment plans based on the patient's specific needs and physiological status through real-time monitoring and data analysis.

The combination of precision therapy and self-powered wearable sensors has shown significant potential in various applications. One common application is wound treatment. Fig. 12(a) depicts a "smart" bandage that utilizes multi-mode wearable devices for physiological monitoring and active

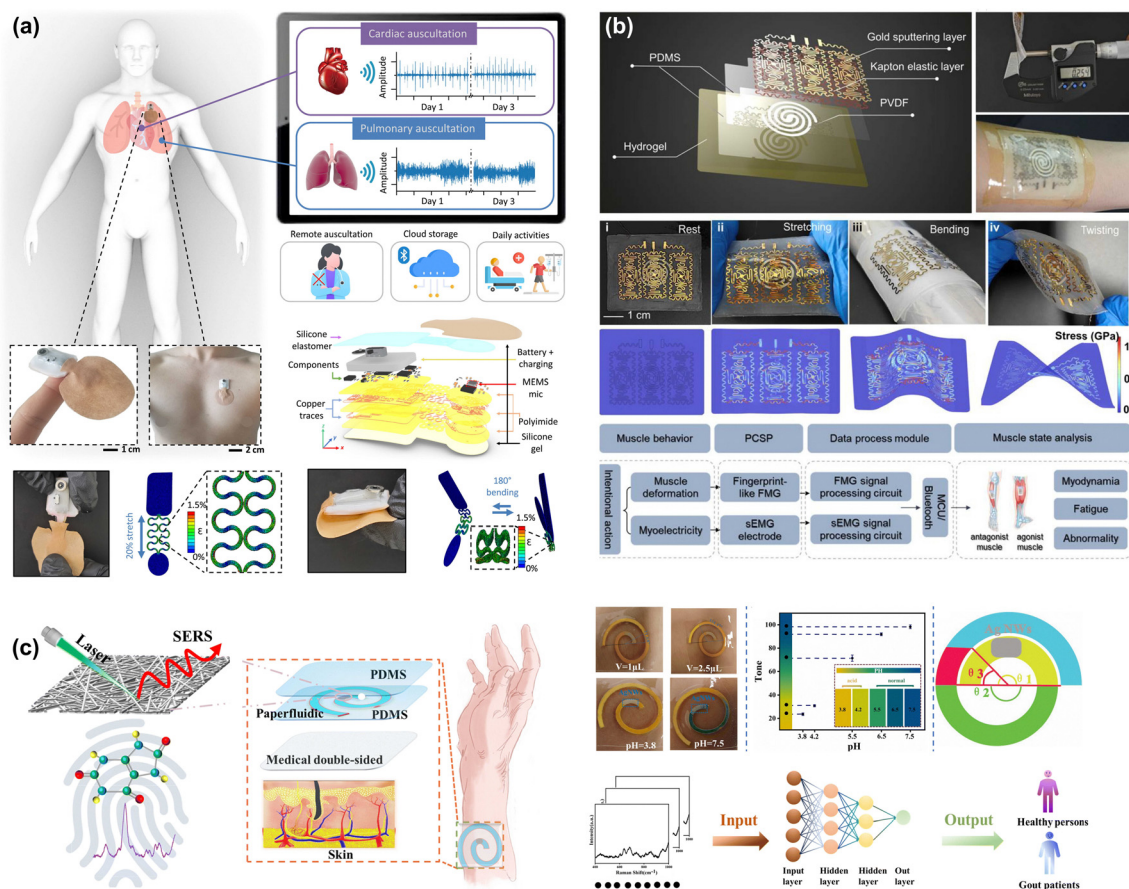


**Fig. 11** Intelligent diagnosis. (a) Schematic illustration of remote monitoring using the SWS, with the zoomed-in photo of the device on the finger and the chest. Exploded view of the SWS with multiple layers of deposited materials. Image of the 20% stretched interconnects in the SWS and its finite element analysis results. Photo of the SWS with 180° bending and finite element analysis results showing cyclic bending. Reproduced with permission from ref. 179. Copyright 2022, The American Association for the Advancement of Science. (b) Overview and design of patterned mechanical–electrically coupled sensing patch, exploded, and physical drawings. Physical photos and finite element analysis results in four different states. Reproduced with permission from ref. 180. Copyright 2024 The Author(s). InfoMat published by UESTC and John Wiley & Sons Australia, Ltd. (c) The sketch and detection process of the wearable intelligent sweat platform. Surface-enhanced Raman spectroscopy detection. Various layers of the platform. The photographs of the wearable platform on human skin. The Hue value is extracted from the wearable platform. The structure parameter of the spiral channel and the process of AI analysis. Reproduced with permission from ref. 181. 2024 Copyright Clearance Center, Inc. All rights reserved.

intervention to facilitate the healing of chronic wounds.<sup>184</sup> It has been developed, featuring a closed-loop wireless-powered sensing along with a skin interface hydrogel electrode that can be adhered to and separated on demand. The observations indicate the activation of pro-regenerative genes in monocyte and macrophage populations, potentially improving tissue regeneration and skin recovery.

In addition, self-powered wearable sensors can be applied in treating complex diseases. Rheumatoid arthritis is a widespread autoimmune disease. An integrated smart device has been developed with wearable and reconfigurable features for inflammation monitoring and collaborative treatment of Rheumatoid arthritis (Fig. 12(b)).<sup>185</sup> The integrated smart device shows high capacitance, low impedance, and suitable mechanical properties. In rodent models, impedance sensing has been validated through machine learning models to indicate inflammatory conditions and facilitate diagnosis. The subsequent collaborative treatment results indicated significant symptom

relief and synovitis elimination. The treatment of diseases is often a long process that can lead to muscle loss. In a study targeting the neurodegenerative disease amyotrophic lateral sclerosis, Proietti *et al.*<sup>186</sup> emphasized the use of a soft, lightweight, portable robotic wearable assistant to aid shoulder movements. Participants using the robotic wearable devices showed improved shoulder range of motion during tasks that simulate daily life activities. This device reduces shoulder muscle activity and perceived muscle depletion while increasing endurance.

The combination of precision treatment and self-powered wearable sensors will usher in an important development trend. Technology integration and intelligence will enable sensors to efficiently analyze physiological data and provide personalized feedback. Secondly, personalized medical solutions will be based on users' genetic information and real-time monitoring data. Data interconnectivity will enhance diagnostic accuracy, while remote monitoring and healthcare will

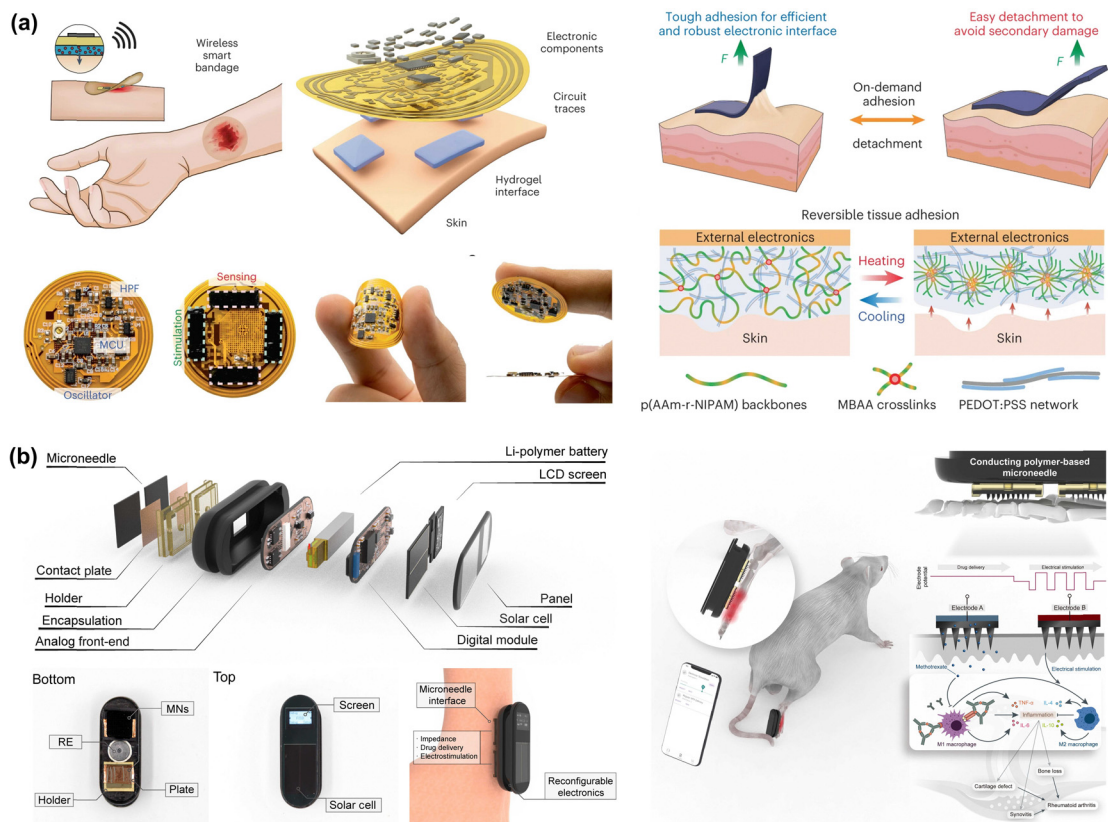


**Fig. 12** Precision treatment. (a) Schematic diagram and exploded view of the wireless smart bandage including FPCB and tissue-interfacing conducting adhesive hydrogels. The schematic diagram for the hydrogel interface in the smart bandage. Schematic diagram illustrating microscopic structural changes during LCST phase transition. Reproduced with permission from ref. 184. Copyright 2022, The Author(s), under exclusive licence to Springer Nature America, Inc. (b) Mechanism of drug and electrical stimulation synergistic therapy using an integrated smart device. Rodent models are used to collect clinical parameters to train and validate machine learning models and to evaluate the outcomes of synergistic treatments. Reproduced with permission from ref. 185. Copyright 2024, The American Association for the Advancement of Science.

improve patient management. Overall, this combination will promote the development of the medical industry towards intelligence and precision.

#### 4.4 Scientific rehabilitation

The combination of scientific rehabilitation and self-powered wearable sensors significantly improves the efficiency and personalization of the rehabilitation process. These sensors can monitor physiological indicators in real-time, provide immediate feedback, and help adjust rehabilitation plans.<sup>175</sup> By collecting data, personalized rehabilitation plans can be developed to enable patients to participate and actively enhance their self-management abilities.<sup>187</sup> In addition, combining AI for data analysis can identify trends and issues and provide intelligent feedback. Overall, this combination optimizes the rehabilitation effect and enhances patients' sense of participation and safety.<sup>188</sup>

The main goal of rehabilitation is to reduce functional impairments caused by illness or injury and help patients return to their daily lives, work, and social activities as much as possible. The knee joint is a vulnerable area in daily life, often susceptible to injuries and strain due to its crucial role in

movement and weight-bearing activities. A magnetically driven piezoelectric cantilever beam generator array effectively harvests energy from human joint motion to power temperature and humidity sensors, while detecting rotation angles and angular velocities (Fig. 13(a)).<sup>45</sup> A wearable joint rehabilitation monitoring system combines this array with wireless data acquisition and software, enabling real-time measurement of joint range of motion and flexion evaluation for effective rehabilitation. Moreover, as technology advances, knee joint detection equipment is continually updated, improving accuracy and effectiveness in monitoring and diagnosing issues. Fig. 13(b) presents a wearable brace designed for the rehabilitation self-assessment of patients undergoing total knee arthroplasty.<sup>41</sup> This system consists of force sensors to measure muscle strength and active angle sensors to detect knee joint curvature. Clinical trials with total knee arthroplasty patients have shown the system's feasibility and significance. Specifically, by utilizing personalized healthcare through the braces, the rehabilitation process is quantified in terms of muscle strength, leading to measurable enhancements in recovery. In addition to these, many exoskeletons and pressure wearable sensors mentioned earlier are scientific rehabilitation devices.

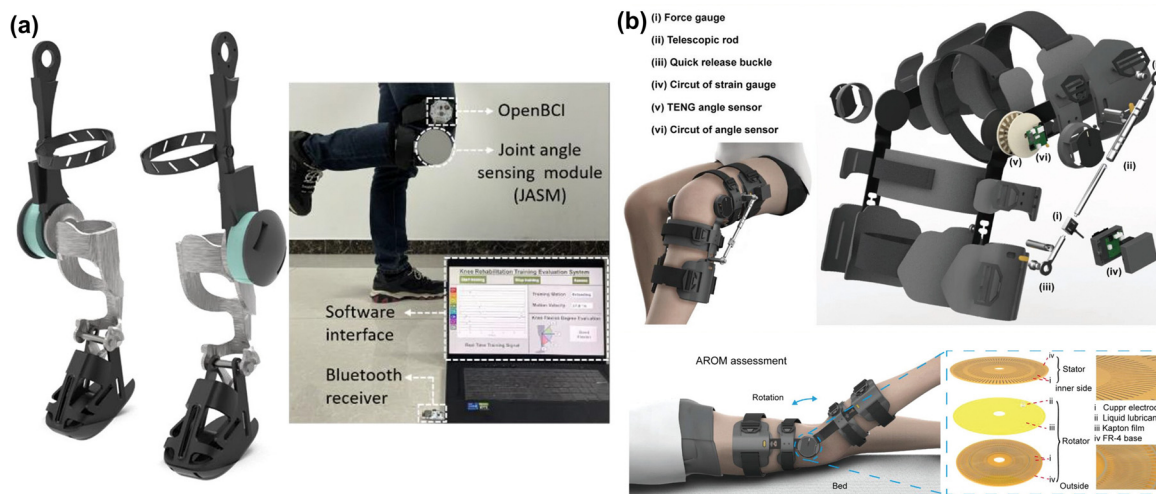


**Fig. 13** Scientific rehabilitation. (a) Schematic diagram of a wearable exoskeleton system for the knee joint and the whole system. Reproduced with permission from ref. 45. Copyright © 2022, American Chemical Society. (b) A perspective view of a brace with a modular device for measuring isometric myodynamia and joint ROM (range of motion). Schematic illustration of active range of movement test and TENG liquid-enhanced angle sensor with interface liquid enhancement. Reproduced with permission from ref. 41. Copyright 2022 The Authors. Advanced Science published by Wiley-VCH GmbH.

By applying AI technology, sensors can adjust training intensity based on monitoring data and provide real-time guidance. Remote rehabilitation support will enhance patient convenience and accessibility, and data integration and analysis will promote collaboration among medical teams. The system will also be able to identify potential health risks, achieve early intervention, and reduce the incidence of complications. Additionally, wearable devices will be more lightweight and comfortable, enhancing the user experience. This combination will promote the development of rehabilitation medicine towards intelligence and personalization, improving patients' rehabilitation outcomes and quality of life.

## 5. Challenges and prospects

Currently, self-powered wearable sensors are making significant advancements in the field of digital health and are transforming the way health monitoring and management are

carried out.<sup>189</sup> However, this technology also faces several challenges, including improving sensor sensitivity, achieving device miniaturization, enhancing self-powered efficiency, optimizing remote communication control, and integrating multifunctional capabilities and AI applications.<sup>190</sup> Addressing these issues will not only enhance the practicality and user experience of devices but also improve the accuracy and real-time performance of health data, thereby promoting the broader development of self-powered wearable sensors in the medical domain (Fig. 14).<sup>161</sup>

(1) To improve the sensitivity of self-powered wearable sensors, it is crucial to focus on improving material properties and refining structural design. Advanced materials such as high-sensitivity semiconductors, nanomaterials, or composite materials can greatly enhance the sensor's response to specific signals due to their superior electrical and mechanical properties at the microscopic level. Moreover, optimizing the structural design of sensors is essential. Increasing the sensor's

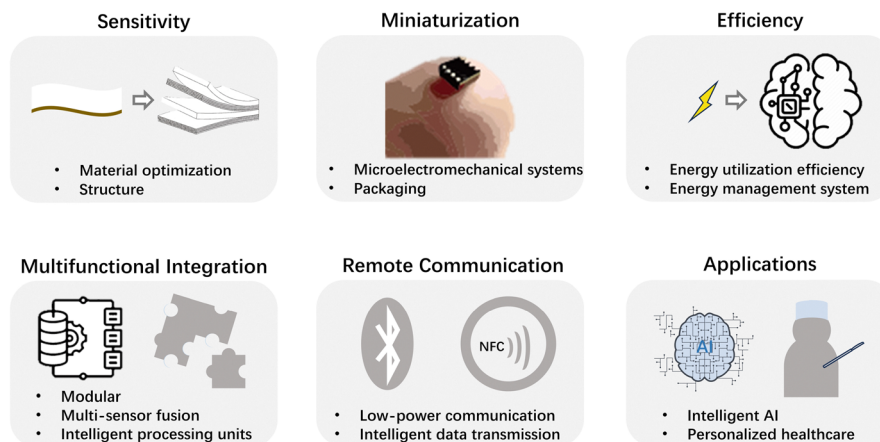


**Fig. 14** The future development roadmap of self-powered wearable sensing devices.

surface area or optimizing its geometry can effectively improve its signal-capturing ability. For instance, utilizing complex shapes through multi-layer structures or 3D printing technology can enhance the contact area with physiological signals, thereby improving sensitivity and response speed. By optimizing both material and structural design, self-powered wearable sensors are expected to significantly improve sensitivity, leading to broader and more effective health monitoring and management applications.

(2) To achieve miniaturization of equipment, in addition to material improvement and sensor design optimization, utilizing advanced preparation techniques and optimizing packaging design are equally crucial. During the preparation process, the use of MEMS technology to manufacture microsensors can achieve both compact and efficient sensor design. This technology significantly reduces the size of sensors while maintaining functionality, making them suitable for the requirements of wearable devices. Despite advancements, MEMSs still encounter significant challenges, including the need for complex multi-layer interconnects and sensor integration in printed circuits. Additionally, there is a critical need to balance size, cost, and scalability to achieve efficient multifunctional integration at the micrometer level. Another effective method is to develop ultra-thin sensors that are easily integrated into clothing or patches. This integration method not only improves portability but also enhances the user's wearing comfort. In addition, optimizing packaging design is equally important, as sensors can be protected through film packaging and 3D packaging technology while maintaining their flexibility. This packaging method not only effectively protects the sensor but also ensures its reliable performance in various environments. In short, through comprehensive optimization of materials, design, and packaging, the miniaturization of devices will greatly enhance the practicality of self-powered wearable sensors, making them better meet the needs and application scenarios of users.

(3) To enhance the efficiency of self-powered equipment, various methods can be utilized, including improving energy utilization and optimizing energy management systems. When it comes to optimizing energy utilization, hybrid power generation methods can be employed by combining nanogenerators with other power sources such as fuel cells and electrochemical methods. This comprehensive use of different energy sources can ensure a stable and efficient power supply for equipment in various environments and application scenarios. Moreover, the development of low-power sensor devices is essential for improving the performance of energy management systems. These low-power devices can maintain efficient monitoring functions while minimizing energy consumption, thereby extending the working time of self-powered devices. Additionally, integrating energy capture, storage, and sensor capabilities into a compact system can effectively reduce losses during energy transmission. This integration can improve the overall efficiency of the system and enhance the reliability and portability of the equipment. In summary, by improving energy utilization and optimizing energy management, the efficiency

of self-powered wearable devices will be significantly enhanced, providing more sustainable and reliable power support for health monitoring and other application areas.

(4) To achieve multifunctional integration, we can use modular design, multi-sensor fusion, and intelligent processing units. Modular design allows for independent design of sensors, communication modules, and energy harvesting modules, facilitating the integration of different functions and enhancing upgrade flexibility. By designing flexible interfaces and communication protocols, seamless integration of different functional modules can be achieved, ensuring overall compatibility and scalability of the system. Integrating multiple sensors can improve the accuracy and reliability of data through data fusion technology, allowing data from different sensors to complement each other and provide more comprehensive health monitoring information. Using computer algorithms to process multi-sensor data can better analyze users' health status and help doctors develop personalized medical plans. The integrated intelligent processing unit can achieve on-site data processing and analysis, reducing dependence on data transmission. Through edge computing technology, the system can conduct real-time data processing and analysis, thus improving the reaction speed and decision-making efficiency. This efficient processing capability not only optimizes the user experience but also enhances the potential application of wearable devices in dynamic health monitoring. In short, through multifunctional integration, self-powered wearable devices will better meet the needs of modern healthcare and health management.

(5) To enhance remote communication control, we can utilize low-power communication design and an intelligent data transmission strategy. The low-power communication design employs technologies like Bluetooth Low Energy or Near Field Communication to reduce device energy consumption and prolong the usage time of wearable sensors. Additionally, low-power wide area network technologies such as Zigbee or LoRa can be utilized to expand communication range and ensure stable data transmission over longer distances. Implementing intelligent data transmission strategies is also crucial. These strategies can dynamically adjust the transmission frequency and optimize based on the importance and urgency of sensor data. For example, using an event-driven transmission mechanism and transmitting data only when necessary can effectively reduce unnecessary communication and save electricity. By combining these approaches, remote communication can improve energy efficiency, ensure the timeliness and reliability of data transmission, and provide users with a better health monitoring experience. In summary, optimizing remote communication control will significantly enhance the practicality and functionality of self-powered wearable sensors.

(6) In the future, the combination of self-powered wearable sensors and intelligent AI will expand the applications in the field of digital health. AI can analyze individuals' lifestyle habits, provide advice on healthy lifestyles, and help people better maintain their health in daily life. For example, individuals can receive personalized advice through AI to promote

healthy daily activities and dietary habits. In terms of physical exercise, AI can analyze sports data, provide feedback on sports performance, and offer improvement suggestions. This allows users to adjust their exercise routine promptly, enhancing their effectiveness. Additionally, AI can create personalized training plans to help users optimize their exercise performance, ensuring that their workouts are both effective and safe. The application of AI is equally crucial in health monitoring and management. By analyzing data from sensors, AI can predict potential health risks and provide personalized health recommendations. Through real-time monitoring of physiological indicators, AI can identify abnormal patterns and issue timely alerts when potential problems are discovered. This intelligent health management not only enhances the monitoring ability of users' health status but also provides necessary interventions at critical moments, further improving users' quality of life. In short, the combination of self-powered wearable sensors and intelligent AI will bring revolutionary changes to the field of digital health, enabling individuals to more actively manage their health and enjoy more personalized and efficient health services.

## 6. Conclusions

This extensive review provides an in-depth exploration of the various power supply methods, structural forms, and diverse applications of self-powered wearable sensors within the digital health domain. The detailed analysis encompasses the influence of structural design, material enhancements, and ongoing advancements in AI on the practical implementation of self-powered wearable sensors. It advocates for further innovation and refinement of self-powered wearable sensors to effectively cater to the evolving needs of future users. In summary, this review underscores the substantial impact of self-powered wearable sensors on the progression of digital health.

## Author contributions

Yumeng Zhang: investigation, article analysis, writing original draft. Engui Wang: revision of the manuscript, editing. Han Ouyang: writing, reviewing & editing. Zhou Li: supervision and funding acquisition.

## Data availability

No primary research results, software or codes have been included and no new data were generated or analysed as part of this review.

## Conflicts of interest

There are no conflicts to declare.

## Acknowledgements

This project is supported by National Key Research and Development Program of China grant (2023YFC2411901); National Natural Science Foundation of China grants (52373256), (T2125003), (62004010); Youth Innovation Promotion Association CAS grant (2023176); Beijing Natural Science Foundation grants (7232347) and (L212010); Beijing Nova Program grant (2024047); Fundamental Research Funds for the Central Universities grant (E0EG6802X2), and grant (E2E45101X2).

## Notes and references

- 1 Q. Du, S. Su, H. Dai and Z. Li, *Chin. Sci. Bull.*, 2024, **69**, 2008–2014.
- 2 T. Lang, *Science*, 2011, **331**, 714–717.
- 3 Y. Xi, S. Cheng, S. Chao, Y. Hu, M. Cai, Y. Zou, Z. Liu, W. Hua, P. Tan, Y. Fan and Z. Li, *Nano Res.*, 2023, **16**, 11674–11681.
- 4 X. Yuan, T. Puchuan, L. Zhou and F. Yubo, *Soft Sci.*, 2023, **3**, 26.
- 5 Y. Lu, D. Kong, G. Yang, R. Wang, G. Pang, H. Luo, H. Yang and K. Xu, *Adv. Sci.*, 2023, **10**, 2303949.
- 6 S. Xu, J. Kim, J. R. Walter, R. Ghaffari and J. A. Rogers, *Sci. Transl. Med.*, 2022, **14**, eabn6036.
- 7 J. Kim, A. S. Campbell, B. E.-F. de Ávila and J. Wang, *Nat. Biotechnol.*, 2019, **37**, 389–406.
- 8 A. Alagumalai, W. Shou, O. Mahian, M. Aghbashlo, M. Tabatabaei, S. Wongwises, Y. Liu, J. Zhan, A. Torralba, J. Chen, Z. Wang and W. Matusik, *Joule*, 2022, **6**, 1475–1500.
- 9 N. Ha, K. Xu, G. Ren, A. Mitchell and J. Z. Ou, *Adv. Intell. Syst.*, 2020, **2**, 2000063.
- 10 K. Xu, Z. Cai, H. Luo, Y. Lu, C. Ding, G. Yang, L. Wang, C. Kuang, J. Liu and H. Yang, *ACS Nano*, 2024, **18**, 26435–26476.
- 11 H. Ouyang, Z. Li, M. Gu, Y. Hu, L. Xu, D. Jiang, S. Cheng, Y. Zou, Y. Deng, B. Shi, W. Hua, Y. Fan, Z. Li and Z. Wang, *Adv. Mater.*, 2021, **33**, 2102302.
- 12 Y. Yang, R. Luo, S. Chao, J. Xue, D. Jiang, Y. H. Feng, X. D. Guo, D. Luo, J. Zhang, Z. Li and Z. L. Wang, *Nat. Commun.*, 2022, **13**, 6908.
- 13 M. Smuck, C. A. Odonkor, J. K. Wilt, N. Schmidt and M. A. Swiernik, *npj Digit. Med.*, 2021, **4**, 45.
- 14 A. Awad, S. J. Trenfield, T. D. Pollard, J. J. Ong, M. Elbadawi, L. E. McCoubrey, A. Goyanes, S. Gaisford and A. W. Basit, *Adv. Drug Delivery Rev.*, 2021, **178**, 113958.
- 15 S. Wang, L. Lin and Z. L. Wang, *Nano Energy*, 2015, **11**, 436–462.
- 16 H. Luo, Y. Lu, Y. Xu, G. Yang, S. Cui, D. Han, Q. Zhou, X. Ouyang, H. Yang, T. Cheng and K. Xu, *Nano Energy*, 2022, **103**, 107803.
- 17 Y. Wang, P. Zhu, Y. Sun, P. Li and Y. Mao, *Bio-Des. Manuf.*, 2024, **7**, 566–590.
- 18 Z. L. Wang and J. Song, *Science*, 2006, **312**, 242–246.
- 19 Z. L. Wang, *MRS Bull.*, 2007, **32**, 109–116.

- 20 G. Prestopino, R. Pezzilli, N. J. Calavita, C. Leonardi, C. Falconi and P. G. Medaglia, *Nano Energy*, 2023, **118**, 109017.
- 21 Y. Shan, E. Wang, X. Cui, Y. Xi, J. Ji, J. Yuan, L. Xu, Z. Liu and Z. Li, *Adv. Funct. Mater.*, 2024, **34**, 2400295.
- 22 J. Nie, X. Chen and Z. L. Wang, *Adv. Funct. Mater.*, 2019, **29**, 1806351.
- 23 K. Maity and D. Mandal, *ACS Appl. Mater. Interfaces*, 2018, **10**, 18257–18269.
- 24 Y. Zheng, T. Liu, J. Wu, T. Xu, X. Wang, X. Han, H. Cui, X. Xu, C. Pan and X. Li, *Adv. Mater.*, 2022, **34**, 2202238.
- 25 A. Subhramaniyan Rasappan, R. Palanisamy, V. Thangamuthu, M. Natarajan, D. Velauthapillai and J. Kim, *Nano Energy*, 2023, **112**, 108490.
- 26 J. Lv, J. Chen and P. S. Lee, *SusMat*, 2021, **1**, 285–302.
- 27 S. Kee, M. A. Haque, D. Corzo, H. N. Alshareef and D. Baran, *Adv. Funct. Mater.*, 2019, **29**, 1905426.
- 28 M. Zadan, A. Wertz, D. Shah, D. K. Patel, W. Zu, Y. Han, J. Gelorme, H. J. Mea, L. Yao, M. H. Malakooti, S. H. Ko, N. Kazem and C. Majidi, *Adv. Funct. Mater.*, 2024, **34**, 2404861.
- 29 Y. Zou, L. Bo and Z. Li, *Fundam. Res.*, 2021, **1**, 364–382.
- 30 Y. Jiang, K. Dong, X. Li, J. An, D. Wu, X. Peng, J. Yi, C. Ning, R. Cheng, P. Yu and Z. L. Wang, *Adv. Funct. Mater.*, 2021, **31**, 2005584.
- 31 A. A. Jan, S. Kim and S. Kim, *Soft Sci.*, 2024, **4**, 10.
- 32 Y. Wang, P. Chen, Y. Ding, P. Zhu, Y. Liu, C. Wang and C. Gao, *Adv. Funct. Mater.*, 2024, **34**, 2409081.
- 33 W. Yan, C. Ma, X. Cai, Y. Sun, G. Zhang and W. Song, *Nano Energy*, 2023, **108**, 108203.
- 34 P. Parashar, M. K. Sharma, B. K. Nahak, A. Khan, W.-Z. Hsu, Y.-H. Tseng, J. R. Chowdhury, Y.-H. Huang, J.-C. Liao, F.-C. Kao and Z.-H. Lin, *J. Mater. Chem. A*, 2025, **13**, 13750–13762.
- 35 L. Pan, Y. Wang, Q. Jin, D. Wu, L. Zhu, Z. Zhou and M. Zhu, *Chem. Eng. J.*, 2024, **497**, 155671.
- 36 W. Kwak, J. Yin, S. Wang and J. Chen, *FlexMat*, 2024, **1**, 5–22.
- 37 Z. Liu, Y. Hu, X. Qu, Y. Liu, S. Cheng, Z. Zhang, Y. Shan, R. Luo, S. Weng, H. Li, H. Niu, M. Gu, Y. Yao, B. Shi, N. Wang, W. Hua, Z. Li and Z. L. Wang, *Nat. Commun.*, 2024, **15**, 507.
- 38 X. Ke, Y. Duan, Y. Duan, Z. Zhao, C. You, T. Sun, X. Gao, Z. Zhang, W. Xue, X. Liu, Y. Mei, G. Huang and J. Chu, *Device*, 2025, **3**(4), 100650.
- 39 Y. Sun, S. Chao, H. Ouyang, W. Zhang, W. Luo, Q. Nie, J. Wang, C. Luo, G. Ni, L. Zhang, J. Yang, H. Feng, G. Mao and Z. Li, *Sci. Bull.*, 2022, **67**, 1284–1294.
- 40 P. Hyosik, G. Gerald Selasie, N. Simiao, R. Hanjun and L. Ju-Hyuck, *Int. J. Extreme Manuf.*, 2025, **7**, 012006.
- 41 J. Luo, Y. Li, M. He, Z. Wang, C. Li, D. Liu, J. An, W. Xie, Y. He, W. Xiao, Z. Li, Z. L. Wang and W. Tang, *Adv. Sci.*, 2022, **9**, 2105219.
- 42 B. Liu, S. Li, Y. Wen, Z. Xie, M. Zhang, Z. Cheng, D. Liu, C. Jia and F. Sun, *Nano Energy*, 2024, **131**, 110322.
- 43 Z. Kou, C. Zhang, B. Yu, H. Chen, Z. Liu and W. Lu, *Adv. Sci.*, 2024, **11**, 2309050.
- 44 Y. Zou, Y. Gai, P. Tan, D. Jiang, X. Qu, J. Xue, H. Ouyang, B. Shi, L. Li, D. Luo, Y. Deng, Z. Li and Z. L. Wang, *Fundam. Res.*, 2022, **2**, 619–628.
- 45 B. Hu, J. Xue, D. Jiang, P. Tan, Y. Wang, M. Liu, H. Yu, Y. Zou and Z. Li, *ACS Appl. Mater. Interfaces*, 2022, **14**, 36622–36632.
- 46 P. Tan, X. Han, Y. Zou, X. Qu, J. Xue, T. Li, Y. Wang, R. Luo, X. Cui, Y. Xi, L. Wu, B. Xue, D. Luo, Y. Fan, X. Chen, Z. Li and Z. L. Wang, *Adv. Mater.*, 2022, **34**, 2200793.
- 47 Q. Yang, S. Yang, P. Qiu, L. Peng, T.-R. Wei, Z. Zhang, X. Shi and L. Chen, *Science*, 2022, **377**, 854–858.
- 48 L. Miao, S. Zhu, C. Liu, J. Gao, Z. Zhang, Y. Peng, J.-L. Chen, Y. Gao, J. Liang and T. Mori, *Nat. Commun.*, 2024, **15**, 8516.
- 49 Y. Han, H. Tetik and M. H. Malakooti, *Adv. Mater.*, 2024, **36**, 2407073.
- 50 M. Rezaie, Z. Rafiee and S. Choi, *ACS Appl. Mater. Interfaces*, 2024, **16**, 36117–36130.
- 51 S. Ding, T. Saha, L. Yin, R. Liu, M. I. Khan, A.-Y. Chang, H. Lee, H. Zhao, Y. Liu, A. S. Nazemi, J. Zhou, C. Chen, Z. Li, C. Zhang, S. Earney, S. Tang, O. Djassemi, X. Chen, M. Lin, S. S. Sandhu, J.-M. Moon, C. Moonla, P. Nandhakumar, Y. Park, K. Mahato, S. Xu and J. Wang, *Nat. Electron.*, 2024, **7**, 788–799.
- 52 Y. Chen, X. Wan, G. Li, J. Ye, J. Gao and D. Wen, *Adv. Funct. Mater.*, 2024, **34**, 2404329.
- 53 D. Hong, Y.-M. Choi, Y. Jang and J. Jeong, *Int. J. Energy Res.*, 2018, **42**, 3688–3695.
- 54 T. Bu, W. Deng, Y. Liu, Z. L. Wang, X. Chen and C. Zhang, *Adv. Funct. Mater.*, 2024, **34**, 2404007.
- 55 S. Chen, N. Wu, S. Lin, J. Duan, Z. Xu, Y. Pan, H. Zhang, Z. Xu, L. Huang, B. Hu and J. Zhou, *Nano Energy*, 2020, **70**, 104460.
- 56 J. Wang, S. Qian, J. Yu, Q. Zhang, Z. Yuan, S. Sang, X. Zhou and L. Sun, *Nanomaterials*, 2019, **9**, 1304.
- 57 W. Wang, B. Cheng, W. Feng, B. He and S. Liu, *J. Appl. Polym. Sci.*, 2023, **140**, e54261.
- 58 A. Waseem, I. V. Bagal, A. Abdullah, M. A. Kulkarni, H. Thaalbi, J.-S. Ha, J. K. Lee and S.-W. Ryu, *Small*, 2022, **18**, 2200952.
- 59 X. Zhou, K. Parida, O. Halevi, S. Magdassi and P. S. Lee, *Sensors*, 2020, **20**, 6748.
- 60 Y. Zhou, J. He, H. Wang, K. Qi, N. Nan, X. You, W. Shao, L. Wang, B. Ding and S. Cui, *Sci. Rep.*, 2017, **7**, 12949.
- 61 R. Feng, F. Tang, N. Zhang and X. Wang, *ACS Appl. Mater. Interfaces*, 2019, **11**, 38616–38624.
- 62 H. Ma, Q. Liu, P. Cheng, L. Shen, J. Ma, F. Lv, Y. Zhang, Y. Jiang, T. Sun and N. Zhu, *ACS Sens.*, 2021, **6**, 4526–4534.
- 63 M. C. Hartel, D. Lee, P. S. Weiss, J. Wang and J. Kim, *Biosens. Bioelectron.*, 2022, **215**, 114565.
- 64 T. Zhang, Y. Ding, C. Hu, M. Zhang, W. Zhu, C. R. Bowen, Y. Han and Y. Yang, *Adv. Mater.*, 2023, **35**, 2203786.
- 65 J. Zhang, A. Chen, S. Han, Q. Wu, Y. Chen, J. Huang and L. Guan, *ACS Appl. Mater. Interfaces*, 2023, **15**, 45260–45269.
- 66 J. Ma, L. Shen, Y. Jiang, H. Ma, F. Lv, J. Liu, Y. Su and N. Zhu, *Anal. Chem.*, 2022, **94**, 2333–2340.

- 67 T. Sun, L. Shen, Y. Jiang, J. Ma, F. Lv, H. Ma, D. Chen and N. Zhu, *ACS Appl. Mater. Interfaces*, 2020, **12**, 21779–21787.
- 68 J. Choi, D. Kwon, B. Kim, K. Kang, J. Gu, J. Jo, K. Na, J. Ahn, D. Del Orbe, K. Kim, J. Park, J. Shim, J.-Y. Lee and I. Park, *Nano Energy*, 2020, **74**, 104749.
- 69 X. Cao, Y. Xiong, J. Sun, X. Zhu, Q. Sun and Z. L. Wang, *Adv. Funct. Mater.*, 2021, **31**, 2102983.
- 70 H. Chu, J. Xue, D. Luo, H. Zheng and Z. Li, *Adv. Mater. Technol.*, 2024, **9**, 2302068.
- 71 H. Ouyang, Z. Liu, N. Li, B. Shi, Y. Zou, F. Xie, Y. Ma, Z. Li, H. Li, Q. Zheng, X. Qu, Y. Fan, Z. L. Wang, H. Zhang and Z. Li, *Nat. Commun.*, 2019, **10**, 1821.
- 72 X. Pu, M. Liu, X. Chen, J. Sun, C. Du, Y. Zhang, J. Zhai, W. Hu and Z. L. Wang, *Sci. Adv.*, 2017, **3**, e1700015.
- 73 R. Wang, L. Mu, Y. Bao, H. Lin, T. Ji, Y. Shi, J. Zhu and W. Wu, *Adv. Mater.*, 2020, **32**, 2002878.
- 74 Y. Dong, S. Xu, C. Zhang, L. Zhang, D. Wang, Y. Xie, N. Luo, Y. Feng, N. Wang, M. Feng, X. Zhang, F. Zhou and Z. L. Wang, *Sci. Adv.*, 2022, **8**, eadd0464.
- 75 C. Li, R. Luo, Y. Bai, J. Shao, J. Ji, E. Wang, Z. Li, H. Meng and Z. Li, *Adv. Funct. Mater.*, 2024, **34**, 2400277.
- 76 X. Liang, T. Jiang, Y. Feng, P. Lu, J. An and Z. L. Wang, *Adv. Energy Mater.*, 2020, **10**, 2002123.
- 77 H. Ouyang and Z. Li, *Sci. Bull.*, 2019, **64**, 1565–1566.
- 78 L. Wu, J. Xue, J. Meng, B. Shi, W. Sun, E. Wang, M. Dong, X. Zheng, Y. Wu, Y. Li and Z. Li, *Adv. Funct. Mater.*, 2024, **34**, 2316712.
- 79 S. Y. Chung, S. Kim, J.-H. Lee, K. Kim, S.-W. Kim, C.-Y. Kang, S.-J. Yoon and Y. S. Kim, *Adv. Mater.*, 2012, **24**, 6022–6027.
- 80 S. Berger, *Science*, 2021, **373**, 278–279.
- 81 J. Yuan, Y. Zhang, C. Wei and R. Zhu, *Adv. Sci.*, 2023, **10**, 2303114.
- 82 H. Li, D. Zhang, C. Wang, Y. Hao, Y. Zhang, Y. Li, P. Bao and H. Wu, *Small*, 2023, **19**, 2300908.
- 83 W. Ren, Y. Sun, D. Zhao, A. Aili, S. Zhang, C. Shi, J. Zhang, H. Geng, J. Zhang, L. Zhang, J. Xiao and R. Yang, *Sci. Adv.*, 2021, **7**, eabe0586.
- 84 Y. Jang, T.-W. Seo, J. Pak, M. K. Park, J. Ahn, G. C. Jin, S. W. Lee, Y. J. Chung, Y.-B. Choi, C. H. Kwon and J. Cho, *Adv. Energy Mater.*, 2024, **14**, 2401255.
- 85 K. Ji, Z. Liang, P. Wang, Z. Li, Q. Ma and X. Su, *Chem. Eng. J.*, 2024, **495**, 153598.
- 86 S. Yin, X. Liu, T. Kaji, Y. Nishina and T. Miyake, *Biosens. Bioelectron.*, 2021, **179**, 113107.
- 87 Z. Ma, J. Ai, Y. Shi, K. Wang and B. Su, *Adv. Mater.*, 2020, **32**, 2006839.
- 88 D. Jiang, H. Ouyang, B. Shi, Y. Zou, P. Tan, X. Qu, S. Chao, Y. Xi, C. Zhao, Y. Fan and Z. Li, *InfoMat*, 2020, **2**, 1191–1200.
- 89 Y. Gai, E. Wang, M. Liu, L. Xie, Y. Bai, Y. Yang, J. Xue, X. Qu, Y. Xi, L. Li, D. Luo and Z. Li, *Small Methods*, 2022, **6**, 2200653.
- 90 M. Li, Y. Lou, J. Hu, W. Cui, L. Chen, A. Yu and J. Zhai, *Small*, 2024, **20**, 2402009.
- 91 R. Liu, Z. L. Wang, K. Fukuda and T. Someya, *Nat. Rev. Mater.*, 2022, **7**, 870–886.
- 92 Y. Gai, Y. Jiang and Z. Li, *Nano Energy*, 2023, **116**, 108787.
- 93 L. Xu, E. Wang, Y. Kang, D. Fu, L. Luo, Y. Quan, Y. Xi, J. Huang, X. Cui, J. Zeng, D. Jiang, B. Shi, H. Feng, H. Ouyang, C. Chen and Z. Li, *Device*, 2025, 100721, DOI: [10.1016/j.device.2025.100721](https://doi.org/10.1016/j.device.2025.100721).
- 94 D. Jiang, T. Wang, E. Wang, J. Xue, W. Diao, M. Xu, L. Luo, Y. Zhao, X. Yuan, J. Wang, L. Ruan, H. Ouyang, Z. Li and Q. Wang, *Nano Energy*, 2024, **131**, 110257.
- 95 H. Chen, S. Guo, S. Zhang, Y. Xiao, W. Yang, Z. Sun, X. Cai, R. Fang, H. Wang, Y. Xu, J. Wang and Z. Li, *Energy Environ. Mater.*, 2024, **7**, e12654.
- 96 S. R. Barman, S.-W. Chan, F.-C. Kao, H.-Y. Ho, I. Khan, A. Pal, C.-C. Huang and Z.-H. Lin, *Sci. Adv.*, 2023, **9**, eadc8758.
- 97 J. Han, J. Li, X. Zhang, L. Zhao and C. Wang, *Chem. Eng. J.*, 2024, **489**, 151493.
- 98 D. Jiang, M. Xu and Q. Wang, Self-Powered Textile Triboelectric Pulse Sensor for Cardiovascular Monitoring, *2023 45th Annual International Conference of the IEEE Engineering in Medicine & Biology Society Articles*, 2023, <https://ieeexplore.ieee.org/document/10340694>.
- 99 S. Wang, M. He, B. Weng, L. Gan, Y. Zhao, N. Li and Y. Xie, *Nanomaterials*, 2018, **8**, 657.
- 100 R. Hinchet, H.-J. Yoon, H. Ryu, M.-K. Kim, E.-K. Choi, D.-S. Kim and S.-W. Kim, *Science*, 2019, **365**, 491–494.
- 101 B. Shao, M.-H. Lu, T.-C. Wu, W.-C. Peng, T.-Y. Ko, Y.-C. Hsiao, J.-Y. Chen, B. Sun, R. Liu and Y.-C. Lai, *Nat. Commun.*, 2024, **15**, 1238.
- 102 D.-L. Wen, P. Huang, H.-T. Deng, X.-R. Zhang, Y.-L. Wang and X.-S. Zhang, *Microsyst. Nanoeng.*, 2023, **9**, 94.
- 103 H. Ouyang, J. Tian, G. Sun, Y. Zou, Z. Liu, H. Li, L. Zhao, B. Shi, Y. Fan, Y. Fan, Z. L. Wang and Z. Li, *Adv. Mater.*, 2017, **29**, 1703456.
- 104 A. Ghaffarinejad, X. García-Casas, F. Núñez-Gálvez, J. Budagosky, V. Godinho, C. López-Santos, J. R. Sánchez-Valencia, Á. Barranco and A. Borrás, *Device*, 2025, **3**, 100566.
- 105 J. Li, W. Qu, J. Daniels, H. Wu, L. Liu, J. Wu, M. Wang, S. Checchia, S. Yang, H. Lei, R. Lv, Y. Zhang, D. Wang, X. Li, X. Ding, J. Sun, Z. Xu, Y. Chang, S. Zhang and F. Li, *Science*, 2023, **380**, 87–93.
- 106 H.-Y. Zhang, Y.-Y. Tang, Z.-X. Gu, P. Wang, X.-G. Chen, H.-P. Lv, P.-F. Li, Q. Jiang, N. Gu, S. Ren and R.-G. Xiong, *Science*, 2024, **383**, 1492–1498.
- 107 Z.-X. Huang, L.-W. Li, Y.-Z. Huang, W.-X. Rao, H.-W. Jiang, J. Wang, H.-H. Zhang, H.-Z. He and J.-P. Qu, *Nat. Commun.*, 2024, **15**, 819.
- 108 Y. Su, W. Li, X. Cheng, Y. Zhou, S. Yang, X. Zhang, C. Chen, T. Yang, H. Pan, G. Xie, G. Chen, X. Zhao, X. Xiao, B. Li, H. Tai, Y. Jiang, L.-Q. Chen, F. Li and J. Chen, *Nat. Commun.*, 2022, **13**, 4867.
- 109 Y. Bai, H. Meng, Z. Li and Z. L. Wang, *Med. Mater.*, 2024, **1**, 40–49.
- 110 B. Tian, R. Tian, S. Liu, Y. Wang, S. Gai, Y. Xie, D. Yang, F. He, P. Yang and J. Lin, *Adv. Mater.*, 2023, **35**, 2304262.

- 111 W. Zhu, B. Wu, Z. Lei and P. Wu, *Adv. Mater.*, 2024, **36**, 2313127.
- 112 D. Li, S. Li, C. Zhang and W. Chen, *Int. J. Mech. Sci.*, 2023, **247**, 108201.
- 113 Y. Ren, F. Zhang, Z. Yan and P.-Y. Chen, *Device*, 2025, **3**, 100676.
- 114 Z. Yang, Q. Wang, H. Yu, Q. Xu, Y. Li, M. Cao, R. Dhakal, Y. Li and Z. Yao, *Adv. Sci.*, 2024, **11**, 2401515.
- 115 C. Lang, J. Fang, H. Shao, H. Wang, G. Yan, X. Ding and T. Lin, *Nano Energy*, 2017, **35**, 146–153.
- 116 F. Mokhtari, K. A. S. Usman, J. Zhang, R. Komljenovic, Ž. Simon, B. Dharmasiri, A. Rezk, P. C. Sherrell, L. C. Henderson, R. J. Varley and J. M. Razal, *ACS Appl. Mater. Interfaces*, 2025, **17**, 3214–3228.
- 117 M. Du, Y. Cao, X. Qu, J. Xue, W. Zhang, X. Pu, B. Shi and Z. Li, *Adv. Mater. Technol.*, 2022, **7**, 2101332.
- 118 X. Gao, M. Zheng, M. Zhu and Y. Hou, *Nano Energy*, 2023, **116**, 108773.
- 119 P. Tan, Y. Xi, S. Chao, D. Jiang, Z. Liu, Y. Fan and Z. Li, *Biosensors*, 2022, **12**, 234.
- 120 H. Arisawa, Y. Fujimoto, T. Kikkawa and E. Saitoh, *Nat. Commun.*, 2024, **15**, 6912.
- 121 M. Shen, K. Liu, G. Zhang, Q. Li, G. Zhang, Q. Zhang, H. Zhang, S. Jiang, Y. Chen and K. Yao, *Nat. Commun.*, 2023, **14**, 7907.
- 122 Y. Liu, Q. Zhang, A. Huang, K. Zhang, S. Wan, H. Chen, Y. Fu, W. Zuo, Y. Wang, X. Cao, L. Wang, U. Lemmer and W. Jiang, *Nat. Commun.*, 2024, **15**, 2141.
- 123 H. Ryu and S.-W. Kim, *Small*, 2021, **17**, 1903469.
- 124 H. Liu, Y. Lu, A. Xiang, W. Zhang, W. Kuang, S. Yan, Q. Cao, P. Zhou, W. Hou, F. Liu, H. Zhou, X. Song, Z. Luo, B. Chao, Y. Xiang and K. Liu, *Energy Environ. Sci.*, 2025, **18**, 1801–1811.
- 125 S. Choi, *Batteries*, 2023, **9**, 119.
- 126 Y. Wang, X. Xu, G. Dong, M. Zhang, K. Jiao and D. Y. C. Leung, *Energy Rev.*, 2024, **3**, 100099.
- 127 R. Wang, Z. Du, Z. Xia, J. Liu, P. Li, Z. Wu, Y. Yue, Y. Xiang, J. Meng, D. Liu, W. Xu, X. Tao, G. Tao and B. Su, *Adv. Funct. Mater.*, 2022, **32**, 2107682.
- 128 S. A. Graham, P. Manchi, M. V. Paranjape, A. Kurakula, V. S. Kavarthapu, J. K. Lee and J. S. Yu, *Adv. Funct. Mater.*, 2024, **34**, 2409608.
- 129 M. Mariello, L. Fachechi, F. Guido and M. De Vittorio, *Adv. Funct. Mater.*, 2021, **31**, 2101047.
- 130 Z. Wen, M.-H. Yeh, H. Guo, J. Wang, Y. Zi, W. Xu, J. Deng, L. Zhu, X. Wang, C. Hu, L. Zhu, X. Sun and Z. L. Wang, *Sci. Adv.*, 2016, **2**, e1600097.
- 131 C. Lu, H. Jiang, X. Cheng, J. He, Y. Long, Y. Chang, X. Gong, K. Zhang, J. Li, Z. Zhu, J. Wu, J. Wang, Y. Zheng, X. Shi, L. Ye, M. Liao, X. Sun, B. Wang, P. Chen, Y. Wang and H. Peng, *Nature*, 2024, **629**, 86–91.
- 132 M. Chen, X. Li, W. Cai, X. Han, C. Zhou, K. Zheng, R. Duan, Y. Zhao, M. Shao, W. Wang, K. Zheng, B. Feng and X. Shi, *Chin. Chem. Lett.*, 2024, 110712, DOI: [10.1016/j.cclet.2024.110712](https://doi.org/10.1016/j.cclet.2024.110712).
- 133 Z. Wei, Y. Luo, W. Yu, Y. Zhang, J. Cai, C. Xie, J. Chang, Q. Huang, X. Xu, Y. Deng and Z. Zheng, *Adv. Mater.*, 2024, **36**, 2406386.
- 134 W. Zhang, X. Wang, J. Duan, Z. Zheng, J. Zhang, G. Hang and Z. Liu, *ACS Appl. Electron. Mater.*, 2024, **6**, 5429–5455.
- 135 Y. Gao, C. Xie and Z. Zheng, *Adv. Energy Mater.*, 2020, **11**, 2002838.
- 136 F. Mo, G. Liang, Z. Huang, H. Li, D. Wang and C. Zhi, *Adv. Mater.*, 2020, **32**, 1902151.
- 137 C. Chen, S. Ding and J. Wang, *Nat. Med.*, 2023, **29**, 1623–1630.
- 138 B. Dai, C. Gao and Y. Xie, *View*, 2022, **3**, 20220027.
- 139 T. Kirstein, in *Multidisciplinary Know-How for Smart-Textiles Developers*, ed. T. Kirstein, Woodhead Publishing, 2013, pp. 1–25, DOI: [10.1533/9780857093530.1](https://doi.org/10.1533/9780857093530.1).
- 140 Y. Li and Y. Luo, *Science*, 2024, **384**, 29–30.
- 141 J. Peng, F. Ge, W. Han, T. Wu, J. Tang, Y. Li and C. Wang, *J. Mater. Sci. Technol.*, 2025, **212**, 272–280.
- 142 F. Mokhtari, J. Foroughi, T. Zheng, Z. Cheng and G. M. Spinks, *J. Mater. Chem. A*, 2019, **7**, 8245–8257.
- 143 F. Mokhtari, *Self-powered smart fabrics for wearable technologies/Fatemeh Mokhtari*, Springer Nature, Switzerland AG, Cham, Switzerland, 2022.
- 144 F. Mokhtari, Z. Cheng, R. Raad, J. Xi and J. Foroughi, *J. Mater. Chem. A*, 2020, **8**, 9496–9522.
- 145 X. Zhang, W. Lu, G. Zhou and Q. Li, *Adv. Mater.*, 2020, **32**, 1902028.
- 146 J. Zhou, G. Tian, G. Jin, Y. Xin, R. Tao and G. Lubineau, *Adv. Funct. Mater.*, 2020, **30**, 1907316.
- 147 H. J. Sim, C. Choi, C. J. Lee, Y. T. Kim, G. M. Spinks, M. D. Lima, R. H. Baughman and S. J. Kim, *Adv. Eng. Mater.*, 2015, **17**, 1270–1275.
- 148 S. Anand, N. Soin, T. H. Shah and E. Siores, *IOP Conf. Ser.: Mater. Sci. Eng.*, 2016, **141**, 012001.
- 149 X. Chen, Y. He, M. Tian, L. Qu, T. Fan and J. Miao, *Small*, 2024, **20**, 2308404.
- 150 F. Mokhtari, M. Shamshirsaz, M. Latifi and J. Foroughi, *Polymers*, 2020, **12**, 2697.
- 151 K. Zhang, X. Shi, H. Jiang, K. Zeng, Z. Zhou, P. Zhai, L. Zhang and H. Peng, *Nat. Protoc.*, 2024, **19**, 1557–1589.
- 152 F. Mokhtari, G. M. Spinks, S. Sayyar, Z. Cheng, A. Ruhparwar and J. Foroughi, *Adv. Mater. Technol.*, 2021, **6**, 2000841.
- 153 F. Mokhtari, G. M. Spinks, C. Fay, Z. Cheng, R. Raad, J. Xi and J. Foroughi, *Adv. Mater. Technol.*, 2020, **5**, 1900900.
- 154 C. Wei, R. Cheng, C. Ning, X. Wei, X. Peng, T. Lv, F. Sheng, K. Dong and Z. L. Wang, *Adv. Funct. Mater.*, 2023, **33**, 2303562.
- 155 J. Wu, X. Zhou, J. Luo, J. Zhou, Z. Lu, Z. Bai, Y. Fan, X. Chen, B. Zheng, Z. Wang, L. Wei and Q. Zhang, *Adv. Sci.*, 2024, **11**, 2401109.
- 156 Y. Kong, H. Jin, G. Zhang and B. Yuan, *Chem. Eng. J.*, 2024, **496**, 154158.
- 157 F. Alshabouna, H. S. Lee, G. Barandun, E. Tan, Y. Cotur, T. Asfour, L. Gonzalez-Macia, P. Coatsworth, E. Núñez-Bajo, J.-S. Kim and F. Güder, *Mater. Today*, 2022, **59**, 56–67.

- 158 J. Chen, T. He, Z. Du and C. Lee, *Nano Energy*, 2023, **117**, 108898.
- 159 X. Zhang, J. Liang, K. Ahmad, Z. Almutairi and C. Wan, *Device*, 2024, **2**, 100316.
- 160 P. Wang, M. Hu, H. Wang, Z. Chen, Y. Feng, J. Wang, W. Ling and Y. Huang, *Adv. Sci.*, 2020, **7**, 2001116.
- 161 K. Bayoumy, M. Gaber, A. Elshafeey, O. Mhaimed, E. H. Dineen, F. A. Marvel, S. S. Martin, E. D. Muse, M. P. Turakhia, K. G. Tarakji and M. B. Elshazly, *Nat. Rev. Cardiol.*, 2021, **18**, 581–599.
- 162 S. Saifi, X. Xiao, S. Cheng, H. Guo, J. Zhang, P. Müller-Buschbaum, G. Zhou, X. Xu and H.-M. Cheng, *Nat. Commun.*, 2024, **15**, 6546.
- 163 R. Zou, H. Chen, H. Pan, H. Zhang, L. Kong, Z. Zhang, Z. Xiang, J. Zhi and Y. Xu, *Device*, 2024, **2**, 100466.
- 164 Z. Bai, Y. Xu, C. Lee and J. Guo, *Adv. Funct. Mater.*, 2021, **31**, 2104365.
- 165 L. Xing, X. Wang, M. Li, Y. Jia, G. Yang, C. Liu, C. Shen and X. Liu, *Adv. Nanocomposites*, 2024, **1**, 171–179.
- 166 Z. Li, B. Xu, J. Han, J. Huang and H. Fu, *Adv. Funct. Mater.*, 2022, **32**, 2106731.
- 167 J. Huang, S. Peng, J. Gu, G. Chen, J. Gao, J. Zhang, L. Hou, X. Yang, X. Jiang and L. Guan, *Mater. Horiz.*, 2020, **7**, 2085–2096.
- 168 G. Luo, J. Xie, J. Liu, Y. Luo, M. Li, Z. Li, P. Yang, L. Zhao, K. Wang, R. Maeda and Z. Jiang, *Small*, 2024, **20**, 2306318.
- 169 W. Deng, Y. Sun, X. Yao, K. Subramanian, C. Ling, H. Wang, S. S. Chopra, B. B. Xu, J.-X. Wang, J.-F. Chen, D. Wang, H. Amancio, S. Pramana, R. Ye and S. Wang, *Adv. Sci.*, 2022, **9**, 2102189.
- 170 Z. Wu, H. Wang, Q. Ding, K. Tao, W. Shi, C. Liu, J. Chen and J. Wu, *Adv. Funct. Mater.*, 2023, **33**, 2300046.
- 171 N. Kasoju, N. S. Remya, R. Sasi, S. Sujesh, B. Soman, C. Kesavadas, C. V. Muraleedharan, P. R. H. Varma and S. Behari, *CSI Transactions on ICT*, 2023, vol. 11, pp. 11–30.
- 172 A. Labrique, S. Agarwal, T. Tamrat and G. Mehl, *npj Digit. Med.*, 2020, **3**, 120.
- 173 W. Heng, S. Yin, J. Min, C. Wang, H. Han, E. Shirzaei Sani, J. Li, Y. Song, H. B. Rossiter and W. Gao, *Science*, 2024, **385**, 954–961.
- 174 J. He and T. Wang, *Heliyon*, 2023, **9**, e14992.
- 175 A. A. Smith, R. Li and Z. T. H. Tse, *Sci. Rep.*, 2023, **13**, 4998.
- 176 M. C. Roberts, K. E. Holt, G. Del Fiol, A. A. Baccarelli and C. G. Allen, *Nat. Med.*, 2024, **30**, 1865–1873.
- 177 S. Kaur, J. Singla, L. Nkenyereye, S. Jha, D. Prashar, G. P. Joshi, S. El-Sappagh, M. S. Islam and S. M. R. Islam, *IEEE Access*, 2020, **8**, 228049.
- 178 A. Haleem, M. Javaid, R. P. Singh and R. Suman, *Sens. Int.*, 2021, **2**, 100117.
- 179 S. H. Lee, Y.-S. Kim, M.-K. Yeo, M. Mahmood, N. Zavanelli, C. Chung, J. Y. Heo, Y. Kim, S.-S. Jung and W.-H. Yeo, *Sci. Adv.*, 2022, **8**, eabo5867.
- 180 J. Xue, Y. Zou, Z. Wan, M. Liu, Y. Wang, H. Chu, P. Tan, L. Wu, E. Wang, H. Ouyang, Y. Deng and Z. Li, *InfoMat*, 2024, **7**, e12631.
- 181 Z. Chen, W. Wang, H. Tian, W. Yu, Y. Niu, X. Zheng, S. Liu, L. Wang and Y. Huang, *Lab Chip*, 2024, **24**, 1996–2004.
- 182 M. T. Manzari, Y. Shamay, H. Kiguchi, N. Rosen, M. Scaltriti and D. A. Heller, *Nat. Rev. Mater.*, 2021, **6**, 351–370.
- 183 K. M. Abubeker, R. Ramani, K. Raja, G. Sreenivasulu, S. Baskar, M. Sathish, C. Girinivasan and S. Kamalraj, *Sci. Rep.*, 2024, **14**, 6151.
- 184 Y. Jiang, A. A. Trotsyuk, S. Niu, D. Henn, K. Chen, C.-C. Shih, M. R. Larson, A. M. Mermin-Bunnell, S. Mittal, J.-C. Lai, A. Saberi, E. Beard, S. Jing, D. Zhong, S. R. Steele, K. Sun, T. Jain, E. Zhao, C. R. Neimeth, W. G. Viana, J. Tang, D. Sivaraj, J. Padmanabhan, M. Rodrigues, D. P. Perrault, A. Chattopadhyay, Z. N. Maan, M. C. Leeolou, C. A. Bonham, S. H. Kwon, H. C. Kussie, K. S. Fischer, G. Gurusankar, K. Liang, K. Zhang, R. Nag, M. P. Snyder, M. Januszzyk, G. C. Gurtner and Z. Bao, *Nat. Biotechnol.*, 2023, **41**, 652–662.
- 185 Y. Liu, W. Xie, Z. Tang, Z. Tan, Y. He, J. Luo and X. Wang, *Sci. Adv.*, 2024, **10**, eadj0604.
- 186 T. Proietti, C. O'Neill, L. Gerez, T. Cole, S. Mendelowitz, K. Nuckols, C. Hohimer, D. Lin, S. Paganoni and C. Walsh, *Sci. Transl. Med.*, 2023, **15**, eadd1504.
- 187 A. Abedi, T. J. F. Colella, M. Pakosh and S. S. Khan, *npj Digit. Med.*, 2024, **7**, 25.
- 188 Z. Zong and Y. Guan, *J. Knowl. Econ.*, 2024, **16**, 864–903.
- 189 J. V. Vaghasiya, C. C. Mayorga-Martinez and M. Pumera, *npj Flexible Electron.*, 2023, **7**, 26.
- 190 J.-H. Lee, K. Cho and J.-K. Kim, *Adv. Mater.*, 2024, **36**, 2310505.